DESIGN OF A HEAT EXCHANGER FOR WASTE HEAT RECOVERY FROM AN AUTOMOBILE ENGINE AND TO USE IT FOR AIR-CONDITIONING OF THE AUTOMOBILE BY A VAPOUR ABSORPTION SYSTEM

THESIS

SUBMITTED IN PARTIAL FULFILMENT OF THE

REQUIREMENTS FOR THE DEGREE OF MASTER OF MECHANICAL ENGINEERING

Submitted by

ARIJIT BHATTACHARYA

Registration No.: 109151 OF 2009-10

Examination Roll No.: M4MEC1605

Mechanical Engineering Department

Under the Guidance of

PROF. RANAJIT KUMAR CHAKRABORTY

Department of Mechanical Engineering

Faculty of Engineering and Technology

Jadavpur University

Kolkata -700032

India

May, 2016

DECLARATION OF ORIGINALITY AND COMPLIANCE OF ACADEMIC ETHICS

I hereby declare that this thesis contains literature survey and original research work by the undersigned candidate, as part of his Master of Engineering studies.

All information in this document have been obtained and presented in accordance with academic rules and ethical conduct.

I also declare that, as required by these rules and conduct, I have fully cited and referred all material and results that are not original to this work.

Name	: ARIJIT BHATTACHARYA
Examination Roll Number	: M4MEC1605
Registration No	: 109151 OF 2009-10
Class Roll No	: 001411202007
Thesis Title	: Design of a heat exchanger for waste heat recovery from an automobile engine and to use it for air-conditioning of the automobile by a vapour absorption system

Signature :

Date :

Faculty of Engineering and Technology

Department of Mechanical engineering

Jadavpur University

Kolkata-700032

CERTIFICATE OF RECOMMENDATION

I hereby recommend that the thesis entitled **"**Design of a heat exchanger for waste heat recovery from an automobile engine and to use it for air-conditioning of the automobile by a vapour absorption system**"** *prepared under my supervision by Arijit Bhattacharya* (Examination Roll No.- M4MEC1605, Class Roll No.- *001411202007*, Registration No.- 109151 OF 2009-10) *be accepted in partial fulfillment of the requirements for the award of the degree of* ***MASTER OF MECHANICAL ENGINEERING.*** *The matter presented in this thesis has not been submitted in part or full to any other university or institute for the award of any degree.*

……

Prof. Ranajit kumar chakraborty

Thesis advisor

Department of Mechanical Engineering
Jadavpur University

……
.

Prof. Dipankar Sanyal

Professor and head

Department of Mechanical Engineering
Jadavpur University

……

Dean

Faculty of Engineering and Technology
Jadavpur University

Faculty of Engineering and Technology

Department of Mechanical engineering

Jadavpur University

Kolkata-700032

CERTIFICATE OF APPROVAL

The foregoing thesis, entitled as " Design of a heat exchanger for waste heat recovery from an automobile engine and to use it for air-conditioning of the automobile by a vapour absorption system*" is hereby approved by the committee of final examination for evaluation of thesis as a creditable study of an engineering subject carried out and presented by Arijit Bhattacharya (Examination Roll No. M4MEC1605, Class Roll No.001411202007, Registration No. 109151 OF 2009-10) in a manner satisfactory to warrant its acceptance as a pre-requisite to the degree of* ***MASTER OF MECHANICAL ENGINEERING****. It is understood that by this approval, the undersigned do not necessarily endorse or approve any statement made, opinion expressed or conclusion drawn therein, but approve the thesis only for the purpose for which it is submitted.*

Committee on final examination for evaluation of the thesis:

....

....

ACKNOWLEDGEMENT

I express my sincere gratitude to Professor Ranajit Kumar Chakraborty, Department of Mechanical Engineering , Jadavpur University and my project advisor for his valuable guidance and inputs.

I am indebted to Prof. Dipankar Sanyal, Head, Mechanical Engineering Department, Jadavpur University and Prof. Sankar Dhar, Former Head, Mechanical Engineering Department, Jadavpur University for providing the facilities during the course of investigation.

I am also grateful to all the faculty members of Mechanical Engineering Department, Jadavpur University and research scholars of Heat Power laboratory (under Mechanical Engineering Department, Jadavpur University) for their moral support, help and cooperation.

I thank my classmates for the encouragements and help they provided during the project.

I would also like to mention the assistance provided by Mr. Soumik Sengupta , Miss Rakhi Bhattacharya, and Mr. Ranjit Kumar Das and the staffs of the heat power laboratory.

Date: Arijit Bhattacharya

CONTENTS

Abstract

The air conditioning system in a typical automobile car uses vapor compression refrigeration cycle. This cycle requires shaft power to operate and thus reduces the brake power output of the engine and increasing the bsfc. Keeping in view the imminent fuel crisis the world will face in near future, ways to increase the efficiency and bsfc has to be found out to reduce fuel use. Use of vapor absorption refrigeration to air-condition vehicles can use the normally wasted heat content in the exhaust gas to run the air condition system. The present work consists of designing an absorption refrigeration system and a heat exchanger for recovering the exhaust heat. It was seen that plate fin heat exchanger is best suited for this application. The heat thus recovered is used as the input thermal energy to the generator part of the vapor absorption refrigeration system. The heat energy that can be optimally extracted from the exhaust gas and the effectiveness of the heat exchanger was estimated.

Nomenclature

A	Heat transfer surface area	m^2
b_g	Plate spacing in the gas side	m
b_l	Plate spacing in the solution side	m
Bsfc	Brake specific fuel consumption	Kg/bhp.hr
C^*	Heat capacity rate ratio	.....
C_g	Heat capacity rate in the gas side	W/K
C_l	Heat capacity rate in the solution side	W/K
C_{min}	Minimum heat capacity rate	W/K
C_{max}	Maximum heat capacity rate	Kj/hr.K
$c_{p,l}$	Specific heat of cold fluid ($LiBr_2$-H_2O) at constant pressure	Kj/kg.K
$c_{p,g}$	Specific heat of hot fluid (exhaust gas) at constant pressure	Kj/kg.K
D	Mass flow rate of vapor liberated from the generator	Kg/sec
Δp_g	Pressure drops for the fluid flow in gas side	Pa
Δp_l	Pressure drops for the fluid flows in solution side	Pa
δ_g	Fin metal thickness in the gas side	m
δ_l	Fin metal thickness in the solution side	m
δ_w	Wall thickness of the plates	m
ε	Effectiveness of heat exchanger	.....
F	Mass flow rate of strong solution entering into the generator	Kg/sec
f	Specific rich solution circulation rate	.....
h_1, h_2, h_3, h_4	Specific enthalpies	Kj/Kg
G	Mass velocity	kg/m^2s
ξ_{LiBr}	LiBr Concentration in the solution	.....

$K_{c,g}$	Contraction loss coefficient in the gas side	.....
$K_{e,g}$	Loss coefficient due to pressure loss associated with irreversible free expansion in the gas side	
$k_{f,g}$	Thermal conductivity of the fin material (aluminium) in gas side	W /mK
k_l	Thermal conductivity of the $H_2o - Libr$ solutions	W/mK
k_w	Thermal conductivity of the wall material	W/mK
l_g	Fin length for heat conduction in gas side	m
m_g	Fin parameter in gas side	.....
$\dot{m}_g$	Mass flow rate of hot fluid (exhaust gas)	Kg/sec
$\dot{m}_l$	Mass flow rate of cold fluid ($LiBr_2 + H_2O$)	Kg/sec
NTU	Number of (heat) transfer unit	.....
Q_g	Heat transfer in the generator of the absorption unit	KJ
$\eta_{f,g}$	Fin efficiency for gas side	.....
R_w	Wall resistance	K/W
$T_{g,i}$	Hot fluid temperature at inlet of generator	K
$T_{g,o}$	Hot fluid temperature at outlet of generator	K
$T_{l,i}$	Cold fluid temperature at inlet to generator	K
$T_{l,o}$	Cold fluid temperature at outlet to generator	K
$\eta_{o,g}$	Overall surface efficiency in the gas side	.....
U	Overall heat transfer coefficient	W/m^2K
μ	Dynamic viscosity of fluid at average temperature	Pa/s

Introduction

For internal combustion engine, it has been observed that almost 65% of input energy is lost during exhaust. If a part or whole of this energy can be recovered, it will result in saving of power for other systems such as for running an air-conditioning system of the vehicles or for preheating of the suction charge or for running of a supercharger.

It is also important to effectively use the waste heat from the vehicle engines from energy saving and environmental protection point of view.

The objective of the impending work will be:

1. To develop a heat exchanger for capturing waste heat of an engine.
2. To allow the captured heat to run a vapour absorption refrigeration system that will be used to run air conditioning system in a vehicle.
3. To pre-heat the input charge of the engine

As of now, the technologies used for engine waste heat recovery are *(Hatami et al., 2014 —1)*

1. Turbocharging and power turbine
2. Absorption and adsorption refrigeration systems
3. Engine heat exchangers
4. Thermo electric generators
5. Organic Rankine Cycle
6. Six stroke engines
7. Exhaust gas recirculation

In most car engines, waste heat is removed through the radiator by use of a coolant and is rejected to the ambient. The other significant heat rejection is through the exhaust. In high performance automobile engines, a part of the exhaust heat is used for turbo-charging or supercharging. A turbocharger uses a turbine attached to the exhaust system and a supercharger is attached directly to the engine to run a compressor. A number of other techniques, most of which are theoretical, have been proposed to recover the waste heat of an automobile engine.

Turbine is a component which transforms enthalpy into kinetic energy. In a turbocharger, kinetic energy is used to power a compressor. If it is used to

power a generator, it may be called a power turbine. When both the turbocharger and power turbine are used simultaneously then it is called turbo-compounding.

To meet the increasingly stringent engine emission regulation, turbo charging is the most common method to reduce emission and fuel usage.

Nowadays, most of the medium to large size diesel engines have a turbocharger since it increases the mass of air into the engine. By this both drivability and emissions from engines improve. But applications of turbocharger results in higher cylinder back pressure, causing more exhaust gas remaining in the cylinder during exhaust stroke. It is found that optimal thermal efficiency can be achieved only with an appropriate turbo compression ratio (Galindo et al., 1958-1969—2).

Recent studies have been have been focused on the performance of turbocharger and its effects in diesel engines.

Baines et al. (2009—3) analyzed heat transfer phenomena in automobile turbochargers showing series arrangement with the power turbine positioned downstream of the turbocharger. Both types use a bypass valve to control the distribution of the exhaust gas flow rate.

But, for partial loads, low exhaust gas flow rate may prevent satisfactory operation of the power turbine (Dzida and Mucharski., 2009—4).

Also the power turbine makes the strategy to control exhaust distribution between turbocharger and power turbine rather complex.

Refrigeration is needed to meet cooling requirements in air-conditioning, ice-making and medical applications. Mechanical refrigeration system consumes fuel energy or electric energy to achieve either air conditioning or ice making. Use of waste heat as energy source is a promising refrigeration technology. There are many types of refrigeration technology being used in automobiles. Some of these are compression refrigeration, absorption refrigeration, adsorption refrigeration and injection refrigeration.

Absorption and adsorption refrigeration system are run by recovered waste heat energy of the main engine and thus increase the energy conversion efficiency. Therefore, considerable fuel can be saved and the mileage of automobile will increase.

Absorption and adsorption refrigeration system operates almost noiselessly and very little maintenance is required (Wang et al., 2005—5).

The method to produce chilling effect using heat energy as the two fluids (refrigerant and absorbent) are mixed and separated continuously is called absorption refrigeration. The heat source energy when transferred to the strong solution separates refrigerant and absorbent.

During evaporation, the refrigerant takes heat from ambient and lowers its temperature.

Nairn discovered absorption refrigeration in 1777 (Shu et al., 2013—6).

Ferdinand Carre´ built and patented first commercial refrigerator in 1823.

Ammonia refrigerant water absorbent (NH_3–H_2O) and water refrigerant lithium bromide absorbent (H_2O–LiBr) are the most common working fluids today.

Lithium bromide–water refrigeration systems have been much studied and used for many years. Water–ammonia systems also have been studied and have a significant potential for application in many countries.

Wang et al (2005—9) studied viability of a gas-to fluid exhaust heat recovery system to power a NH_3–H_2O absorption refrigeration system in trawler chiller.

Manzela et al (2010—10) analyzed an absorption refrigeration system based on exhaust gas.

Srikhirin et al (2001—11) reviewed and compared a number of absorption refrigeration option.

Fernandez-Seara et al (1998—12) investigated an ammonia–water absorption refrigeration plant for onboard cooling production, with a temperature range from 100°C to 150°C. Synthetic oil was used as heat transfer fluid and results were analyzed to find out the optimum thermal operating conditions which minimize total heat transferring area. Exhaust gas flow rate was controlled by means of a bypass valve.

Power turbine can utilize exhaust heat for heavy duty engines. For example, power turbine can be used as a thermal propulsion device to increase fuel efficiency of ship engines. Power turbine has low capital cost compared to steam power plant. It is also environment friendly and has less manufacturing

time. Two types of arrangements can be done based on the position of the power turbine.

In the first type, the main engine feeds the turbocharger and also the power turbine with the exhaust gas in parallel arrangement. In the second type, the turbocharger and the power turbine are put in series from the diesel engine exhaust gas manifold.

Kececiler et al (2000—13) used geothermal energy from hot Spring in Sivas to do a thermodynamic analysis of the Absorption Refrigeration System (VARS) based on water–lithium bromide. It was shown that the geothermal energy from the said source cannot produce electricity efficiently. But the geothermal resource can be applied for refrigeration in storages at 4 -10℃ with significant economic advantage. It was shown that if temperature of heat source is in range from 50℃ to 200℃ then it is economically suitable for absorption Refrigeration Systems.

Hong et al (2011—14) simulated a new ejector-absorption combined refrigeration system. The heat input to the combined cycles is used to drive one sub-cycle. Part of the heat rejected by the first sub-cycle is used to drive a second sub-cycle. This results in additional refrigerant vapor generation. So the COPs of the combined system are much higher in comparison with that of the conventional single-effect refrigeration system. Nevertheless, the refrigeration systems and cycles are complex and the initial investment in system components is high. Ejector is regarded as a key component in combined cycles and system COP depends strongly on ejector performance.

Every part of the combined cycle system is taken to be a control volume with inlet and outlet fluid, heat transfer and work interactions. The main governing equations for all of the components include mass balance equations, energy balance equations and LiBr mass balance equations. To simplify the model of ejector, some assumptions were made:

1. The working fluid and the other fluid do not mix until they reach the mixing chamber.

2. The velocity of the fluid into ejector and the velocity of the fluid coming out of diffuser are neglected as they are of much lower magnitudes in comparison with the velocity of the fluid in mixing chamber.
3. It is assumed that the working fluid flow is one-dimensional.

4. The pressure of the working fluid is equal to that of the other fluid at inlet of mixing chamber. This pressure is equal to pressure of the secondary fluid coming into ejector.

It is seen that combined ejector-absorption refrigeration cycles can improve the performance of absorption refrigeration cycle when temperature of the heat source is lower than the temperature of conventional double effect VARS but much higher than that is required for conventional single effect VARS.

Optimization of thermal systems is in general done by a thermodynamic analysis. However, the systems optimized with such an approach often are not viable due to economic constraints.

Misra et al (2003—15) used the average cost approach to optimize a water-LiBr single effect vapor absorption refrigeration system for application in air-conditioning sector. It was driven by high pressure hot water. This method makes a detailed exergy analysis and determines the average cost per unit exergy of every internal flows and products appearing in the thermo-economic representation of the system.

Due to plant complexities the mathematical and numerical technique-based optimization of thermal systems is not always feasible. Thus a simplified cost minimization methodology, based on concept of exergetic cost, is used to calculate the economic costs for every internal flows and products of the system under consideration.

The concept of exergetic cost is a thermo-economic optimization technique which combines the thermodynamic and economic analyzing methods to obtain an optimum configuration of a thermal system.

After the costs are calculated, an approximately optimum design configuration was obtained in this study.

Kizilkan et al (2007—16) applied thermo-economic theory to optimize different components of system such as condenser, absorber heat exchanger, generator and evaporator. There are two basic thermoeconomic methods. One is the autonomous method which was developed by Tribus and Evans. This method uses the local unitary cost of exergy entering or leaving a system. The other method called the structural method was developed by Beyer and it uses the unitary costs of exergy loses. In this paper the structural method was used to optimize a $LiBr - H_2o$ vapor absorption refrigeration system. Detail exergy and

cost analysis of the system was done and optimum areas of heat exchangers with their optimal temperatures were determined.

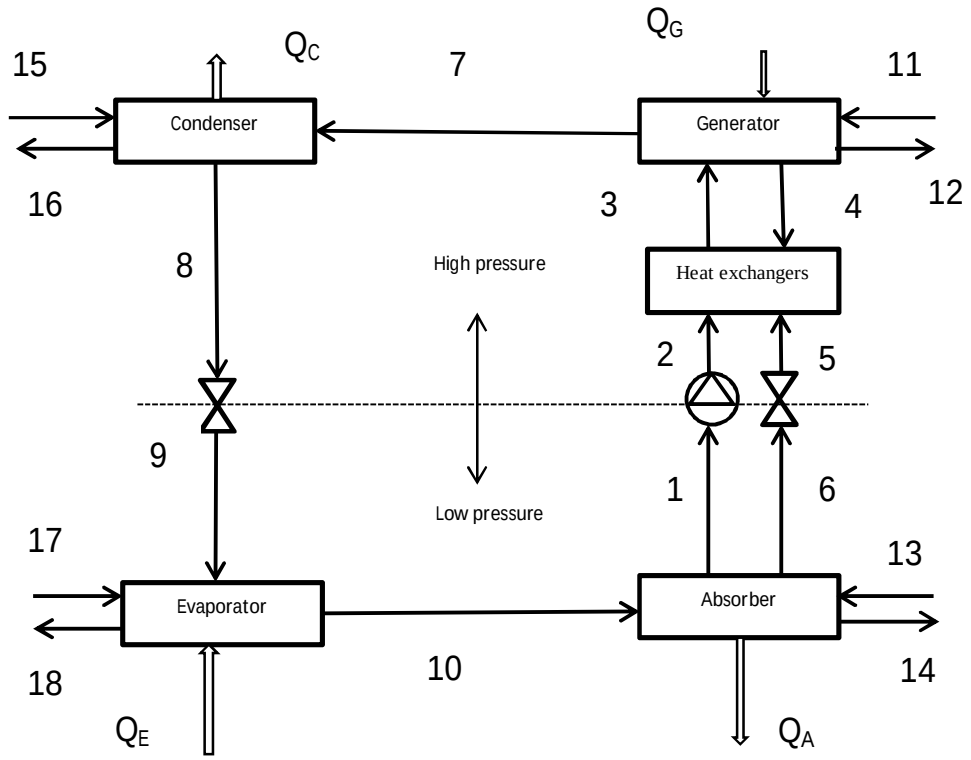

Fig1. Schematic diagram of an absorption refrigeration system.

In the model shown above Q_G and Q_E are the heat input rates from the heat source to the generator and heat input rate from the cooling load to the evaporator respectively. Q_C and Q_A are respectively the heat rejection rates from condenser and absorber to the heat sinks. As shown in Fig. 1, the vapour refrigerant coming from the evaporator (10) is absorbed by liquid solution. This liquid solution is then pumped to a higher pressure (1–2). The refrigerant then boils out from the solution as heat is added (3–7). Then, the refrigerant goes to the condenser (7–8) like in an ordinary cooling cycle. Then the strong LiBr liquid solution returns back to the absorber (6).

For the thermodynamic analysis of the absorption system, the law of mass conservation, first and second laws of thermodynamics are applied to every part of the system. Every part is treated as a control volume with inlet and outlet fluid flows, heat transfers and work interactions. The mass conservation analysis includes the mass balance of each material of the solution. The governing models of mass conservation and every type of material conservation for a steady state and steady flow system are

$$\sum \dot{m}_i - \sum \dot{m}_o = 0$$

$$\sum(\dot{m} \,.\, x)_i - \sum(\dot{m} \,.\, x)_o = 0$$

Where $\dot{m}$ is the mass flow rate and x is mass concentration of LiBr in the solution.

The first law of thermodynamics gives

$$\sum(\dot{m}.\, h)_i - \sum(\dot{m}.\, h)_o + \sum Q_i - \sum Q_o + W = 0$$

An overall energy balance of the system gives

$$Q_C + Q_A = Q_G + Q_E$$

The heat transfer rates of heat exchangers can be written as

$$Q = U \cdot A \cdot \Delta T_{LMTD}$$

The overall heat transfer coefficient U of the heat exchangers was calculated using existing formulae in literature and found out to be about 0.5 W/m^{2}K.

From the exergy balance of the system:

$$\Delta \dot{E}_{IN} = \Delta \dot{I}_T$$

Where $\Delta \dot{E}_{IN} = \dot{E}_{IN} - \dot{E}_{OUT}$ and $\Delta \dot{I}_T$ = total irreversibility of the system

Cost function is taken as the annual cost of system operation and is given by,

$$C_T(x_i) = t_{OP} C_{IN}^{\in} E_{IN}(x_i) + a^C \sum_{l=1}^{n} C_l^C(x_i) + b^C$$

For thermo-economic optimization,

$$\frac{\partial C_T(x_i)}{\partial x_i} = 0$$

From this, the optimization equations were found out.

Talom and Beyene (2008—17) used a 2.8 L internal combustion engine to operate a 3 ton absorption refrigeration system. It was shown that the system is economically feasible.

Garimella et al (2011—18) analyzed a cascaded absorption-vapor compression refrigeration system with a high temperature lift. A single effect LiBr-H_2O and a VRCS using CO_2 as refrigerant were used together. The system provided low temperature refrigeration at -40℃ ,medium refrigeration at 5℃ and medium heat rejection ~55℃ for water heating applications. Thermodynamic analysis showed that the cascaded system has very high cop for a broad range of operations. It was shown that if it is considered that waste heat is free energy, the cop can be as high as 8.

Asdrubali and Grignaffini (2005—19) analyzed the performances of a single step LiBr –H_2O absorption. Source of heat was an electric boiler. All the main operating parameters like temperature, pressure and flow rate were recorded. Performances of the machine with varying flow rate and temperature of hot water were compared with data presented in literature. It was shown that the absorption machine can work effectively when input temperature is about 65℃ − 70℃.

Horuz (1999—20) did an experimental investigation on using vapor absorption refrigeration system in road transport vehicles. Ammonia was used as the refrigerant and water as the absorbent. The experimental device had a cooling

capacity of approximately 10 kW. In the laboratory condition, a anti-freeze (ethylene glycol) solution preventing freezing of water was used as the chilled fluid to allow the system to operate at temperatures below the freezing points of water. It was shown that the system driven by exhaust gas performs the equally in comparison with the gas fired system. A comparative study of the initial and running costs of the conventional refrigeration system and proposed alternative system was done.
The absorber and the condenser were combined in a single conventional finned pipe air-cooled heat exchanger. The generator used was basically a vertical, closed steel cylinder of diameter 15 cm and height 82 cm that is side heated by a natural gas burner. Attached to the top of the generator was a leveling chamber that also contained the rectifier coil. Vapor from the generator flowed into the leveling chamber and hence came into the contact with the rectifier coil, where it was cooled by colder strong solution flowing inside the coil.

Strong and weak solution flow rates in appropriate parts of the system were measured.

The experimental IC engine used was connected to an automatically controlled eddy-current-type dynamometer to simulate different driving conditions. A plenum was built around the existing generator for utilizing the heat from exhaust gases and to link the two systems. The gas flow area of the plenum allowed for two different test cases. In case 1, a large flow area was used, while case 2 had a more restricted flow area. A two-valve arrangement was used in order to regulate the exhaust gas flow to the generator of the VAR system and to isolate the two systems from each other. Isolation would simulate the situation when there was no requirement for exhaust gas to be supplied to the refrigeration system and the exhaust gases would be discharged directly to the surroundings through the normal engine exhaust system.

It was observed that when the engine power output increased, the exhaust gas flow rate increased with increasing speed and load conditions, as would be expected with increasing air and fuel flow. As the engine power output increased, so did the exhaust gas temperature and the exhaust gas heat capacity calculated relative to the ambient temperature also increased. This would be the maximum heat energy recoverable from the exhaust gases at each load/speed condition.

It was seen that the engine cooling water heat capacity is also proportional to the engine power output, but the magnitude is much smaller than the exhaust

gas heat capacity since the maximum cooling water temperature is only about 80°C. This limits the use of engine cooling water as a heat source for the VAR systems using ammonia-water solution.

The change in performance of the IC engine due to introduction of the generator of the VAR system into the engine exhaust system was observed. In case 1, i.e., large free flow area, the engine back pressure is about the same as that of the engine-only tests; hence, the fuel consumption, the exhaust gas temperatures, and the engine efficiency are about the same. But in case 2, it was observed that the engine back pressure is higher than that of engine-only tests because of the more restricted exhaust gas flow area. This caused higher fuel consumption and hence, higher exhausts gas temperature. This higher fuel consumption was equivalent to a 2% reduction in engine efficiency. To avoid this, the gas flow characteristics of the generator and exhaust plenum arrangement of the combined system should be designed to have the same pressure loss characteristics as those of the normal exhaust system.

It was seen that the higher the engine power, the greater was the cooling capacity of the experimental VAR system. This is expected in a VAR system; because the cooling capacity is directly proportional to the heat input to the generator. There was, however, a significant reduction in cooling effect with low engine output. This would affect the unit's performance under slow vehicle speeds or stationary conditions. As power output increased, the heat recovered from exhaust gases also increased. This in turn released an increased quantity of ammonia from the solution in the generator and thus cooling effect was also increased.

A comparison was done on performances of the VARS when fired by natural gas and by engine exhaust gases. It was shown that the performances in two cases were almost same.

Heat exchangers are devices for highly efficiency transfer of thermal energy from one material to another. Heat exchanger can be used separately for waste heat recovery or, can be used in combination with other waste heat recovery devices as organic Rankine cycle and exhaust gas recirculation.

Peyghambarzadeh et al (2011—21) did an experimental investigation on forced convective heat transfer in an automobile radiator with a water based nano-fluid

and compared its performance with that of pure water. The experiment was done using different concentrations of Al_2O_3 nano-particles in water. The number of radiator tubes used was 34. The radiator tubes were of elliptical cross-section and were vertically placed. Liquid flow rate was so changed to have fully turbulent regime with Reynold's number in between $9 * 10^3$ to $2.3 * 10\text{^}4$. The fluid temperature was also varied from 37℃ to 49℃ and effect of it on heat transfer coefficient was studied. It was shown that increase in fluid flow rate improves the heat transfer characteristics. However the effect of fluid inlet temperature was found to be insignificant. It was also found that use of water based nano-fluid can increase the heat transfer efficiency up to 45% with respect to pure water.

Leong et al (2010—22) investigated the application of ethylene glycol based copper nano-fluids in an automobile radiator and shown that it has better heat transfer coefficient and heat transfer rate compared with pure ethylene glycol.

Pandiyarajan et al (2011—23) used a shell and finned tube heat exchanger to recover heat from exhaust gas of an IC engine. A thermal storage tank was used to store the excess energy. By doing so, one problem of waste heat recovery which is its intermittent nature and mismatch between available waste heat energy and demand of it is solved. A combined heat storage tank which stores both latent and sensible energy was made and tests were carried out using phase changing material capsules. It was shown that about 10-15% of fuel energy is stored in the tank and latter can be made available at suitable temperatures.

Zhang and wang (2013—24) studied a finned tube evaporator to extract waste heat from a diesel engine by use of an organic Rankine cycle. The exhaust heat amount from the diesel engine was estimated and heat transfer in the evaporator is roughly estimated for the operating range of engine as speed and load is varied.

Ghazikhani et al (2014—25) used a double pipe counter current heat exchanger for exhaust heat recovery. It is shown that as speed and load of engine increases exergy of recovery heat increases. Use of heat recovery technology is found to be reducing bsfc by about 10%.

Feng Yanget al (2003—26) studied the feasibility of using heat pipes for exhaust gas heat recovery.

Mavridou et al (2010—27) studied the problem of sizing of a heat exchanger. The heat exchanger should be of reasonable size and weight and can handle the

heat load without excessive pressure drop. Five different configurations were investigated. Two groups of configurations which were examined are: (a) a shell and tube heat exchanger with staggered cross-flow tube bundles. Tubes used were smooth circular tubes, finned tubes and tubes with dimpled surfaces. (b)The second configuration was a cross-flow plate heat exchanger. At first tests were done using finned surfaces on the exhaust gas side and then with metal foam material of 10 ppi and 40 ppi as a substitute for the fins. In order to size the heat exchanger for the different configurations, calculations were done using established heat exchanger design methods and data available from literature .The solutions reduced the heat exchanger size. The plate and fin type pressure drop reduction was highest (up to 98% reduction), and the most compact in terms of size and weight was the heat exchanger with 40 ppi metal foam.

Adsorption cooling is a promising alternative to traditional vapor compression refrigeration. The use of adsorption refrigeration in automobiles has many benefits like saving of primary energy sources and reduction in the use of CFCs. Also the cooling system can be powered by engine's waste heat resulting in gas consumption reduction. Adsorption cooling devices have no moving parts, which leads to high reliability and silent operation (Zhang and Wang.,1997—28).

The basic adsorption cycle has a theoretical coefficient of performance of about 0.5.

The viability of adsorption cooling for waste heat recovery application in automobile and in engines was studied by Zhu et al (1992—29) and Suzuki (1993—30).

Zhang and Wang (1997—28) considered a two-bed basic zeolite-water adsorption cycle. In this study, a detailed non-equilibrium dynamic model is developed to estimate the influences of various operating parameters on the performance of the adsorption cooling system for waste heat recovery in the automobile engine. The dynamic nature of the various internal and external interactions between the adsorbent and cooling fluids was discussed. The system comprises of four heat exchangers. These are an air finned forced convection condenser, an air finned forced convection evaporator and a pair of shell and tube type adsorbers. In addition there are four one-way refrigerant valves, an expansion valve, and an exchange valve.

The adsorbent is placed into the adsorber heat exchangers while the refrigerant fluid flows through the steel tubes of the adsorber heat exchangers. Switching of

the exchange valve makes the two adsorbers alternate their functions after an interval so that a continuous supply of chilled air is obtained.

The heating fluid of the adsorbers is engine's hot exhaust gas, and the cold fluid is atmospheric air impelled by a blower. The adsorbent -adsorbate pair used here is zeolite 13x-water. It is used because the regeneration temperature of zeolite 13x-water is high enough for engine's exhaust gas heat recovery. The two adsorbers used were identical. The adsorbers operated in the same cycle but out of phase.

The thermodynamic properties like specific heats of air, absorbate vapor, absorbate liquid and exhaust gas, the latent heat of evaporization and the saturation pressure at adsorbate liquid and vapor equilibrium were written as functions of temperature with the help of the standard formulae available in literature. Using adsorption equations and conservation of energy principle, COP and specific cooling power (SCP) was found out.

It was found that the SCP is more sensitive to parameter changes than the COP. And improving the U*A is the most effective way to obtain an increased SCP, but only in the ranges lower than the threshold value. The threshold value is determined by the overall mass transfer coefficient.

Thermoelectric generators (TEG) or Seebeck generators are systems that can directly generate electrical energy from waste heat energy. These devices are based on the Seebeck effect phenomenon which was first discovered by Thomas Johann Seebeck in 1821. Recently, New types of semiconductor p–n junctions were added to the systems in order to increase the efficiency of these devices. These novel semiconductor p–n junctions are made up from new materials such as BiTe (bismuth telluride), CeFeSb (skutterudite), ZnBe (zinc–beryllium), SiGe (silicon–germanium), SnTe (tin telluride) and new nano-crystalline or nano-wire thermoelectric. These additions increase the efficiency of TEG devices to about 5–8%. TEG devices have many advantages. The energy generated by TEG devices is pollutionless and soundless. TEG devices also do not have any moving component thus requiring much less maintenance costs. However these devices are cost effective only when used with high temperature sources (of the order of 4200 °C) and when only small amounts of power (for example a few milliwatts) are needed. Because of the different advantages of TEG's, many works have been done on its use for automobile waste heat recovery.

Weng and Huang (2013—31) did a simulation of waste heat recovery using thermo-electric generator. It was found that using more number of thermo electric couples do not generate more power in all cases. It is due to rapid drop of exhaust pipe wall temperature. Again as the number of TE couples increases, each TE gets less heat. It was also found that a downstream part of the exhaust pipe is better to be left uncovered. If those parts are not covered with TE couples, then the downstream wall of the pipe will become even hotter than upstream wall of the pipe which is covered with TE couples. Then, heat will be conducted from downstream wall to upstream wall and the upstream TEGs will get more heat resulting in increased heat recovery.

Lu et al (2013—32) showed that the heat recovery by exhaust TEG is dependent on both heat energy and conversion efficiency of TE couples. In order to increase the thermal energy recovery from exhaust gas, highly efficient heat exchangers are required. Heat transfer is combined with pressure drop of heat exchanger in general. Also the muffler for noise reduction creates significant pressure drop. The exhaust heat exchanger was coupled with muffler in the form of 1-inlet 2-outlet, 2-inlet 2-outlet and the baseline empty cavity. A comparison between different vehicle operating conditions was done in respect to thermal uniformity and pressure drop characteristics. It was seen that 1-Inlet 2-outlet improved hydraulic disturbance and heat transfer, and so resulted in an evenly flow distribution and higher surface temperature than the other configurations. But the thermoelectric conversion efficiency was less because of low average surface temperature (<100 °C). It was found that the pressure drops of 1-inlet 2-outlet and 2-inlet 2-outlet were respectively 165% and 318% higher than that of empty cavity configuration for inlet temperature of 100 °C and mass flow rate of 131 kg/h, and were respectively 319% and 523% more than that of empty cavity configuration for inlet temperature of 400 °C and mass flow rate of 156 kg/h.

Love et al (2012—33) did an experimental study on thermoelectrics with clean and fouled heat exchangers and with different materials. The thermoelectrics were tested with a bench-scale thermoelectric heat recovery device simulating automotive exhaust. It was seen that with higher exhaust gas flow, thermoelectric power output increases whereas overall system efficiency decreases from 0.95% to 0.6%.A simulation for reduction of efficiency of EGR-type heat exchangers was also done placing the heat exchangers to diesel engine exhaust in thermophoretic conditions forming a deposit. It is seen that in a

fouled EGR-type heat exchanger, power recovery and overall efficiency is 5–10% lower for all conditions tested.

There are many numbers of thermodynamic cycles available in literature for exhaust waste heat recovery from engines. Some of the important cycles are Calina, trilateral flash, Goswami and Rankine cycle. Out of these, Organic Rankine Cycle (ORC) is the most efficient cycle for heat recovery from low temperature sources such as engine exhaust gas. A schematic of the ORC is shown in Fig.2 which contains boiler, expander, condenser, pump and working fluid (Duparchy et al.,2009—34). Many works are done in this field and complete reviews of them are presented by Sprouse et al.(2013—35), Chen et al. (2010—36) and Wang et al. (2011—37).

Most of these works are based on the effect of working fluid type on the ORC performance. There are different types of working fluids such as wet, dry and isentropic fluids .The T–S diagram slopes of the working fluid can be positive, negative or infinite depending on the type of fluid. The suitable working fluid depends on the operating condition. Maximum efficiency cannot be achieved at all conditions for a particular working fluid.

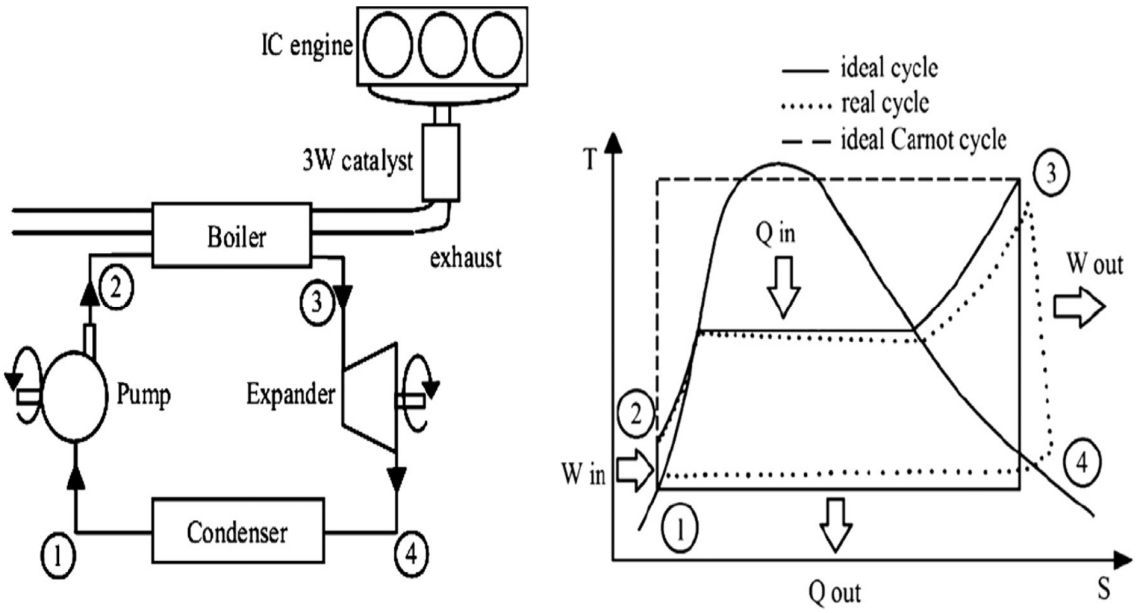

Fig2. Schematic of Organic Rankine Cycle (ORC) on diesel engine and T-S Diagram

Six-stroke engine is a novel type of internal combustion engine. It is mostly based on the principles of the four-stroke engine but with added parts to make the engine more efficient and reduce emission. Three types of six stroke engines have been developed since the1890s (saidur et al., 2012—38). In one of them proposed by Conklin and Szybist (2010—39), the engine extracts the waste heat from the four-stroke diesel engine .This thermal energy is then used to generate additional power without any increase in fuel consumption.

The cycle can be thought of consisting of two power strokes. First power stroke has burnt gas generated from burning of air fuel mixture as working fluid. In the second power stroke, water is injected into the cylinder to extract the waste heat of burned gases and thermal energy contained in the cylinder walls from the previous stroke. Water injection occurs after compressing the burned gases from first stroke when the crank shaft angle is 720°. If the injected water amount is increased, the Mean effective pressure (MEP) of the engines will increase. The main advantage of this engine is reduction in emission. Injected water can also be preheated by using an exhaust heat exchanger.

Recirculation of the exhaust gases into cylinder or EGR is one of the efficient methods to decrease the NO_x emission from automobile. EGR can be used internally or externally in the engines. EGR is widely used in both gasoline and diesel engines(Wei et al.,2012—40),(Zheng et al.,2004—41).

In a diesel engine, the exhaust gas replaces some part of the excess oxygen present in the pre-combustion mixture. Major part of NO_x forms when a mixture of nitrogen and oxygen is injected into high temperature combustion zone. As the EGR lowers the combustion chamber temperature, so the amount of the NOx will reduce in an automobile with EGR system. However, EGR cannot improve the combustion irreversibility and lowers the thermodynamic efficiency of the cycle. It is only a technique to use the thermal energy of burnt gases in the cylinder for another time (Ghazikhani et al.,2010—42).

Scope of work

A vapor absorption refrigeration cycle will be used to recover heat from exhaust gas of an automobile engine and used for air conditioning of the automobile space. A heat exchanger will be designed to extract the maximum possible amount of heat from the exhaust gas. Two types of heat exchangers was found suitable for this heat recovery application, namely, plate fin heat exchanger and plate and frame heat exchanger. Design and performance calculation of both types of heat exchanger is to be done. The heat exchanger to be designed is a cross-flow type heat exchanger.

This heat exchanger will act as the generator of the vapor absorption cycle (Fig. 3)

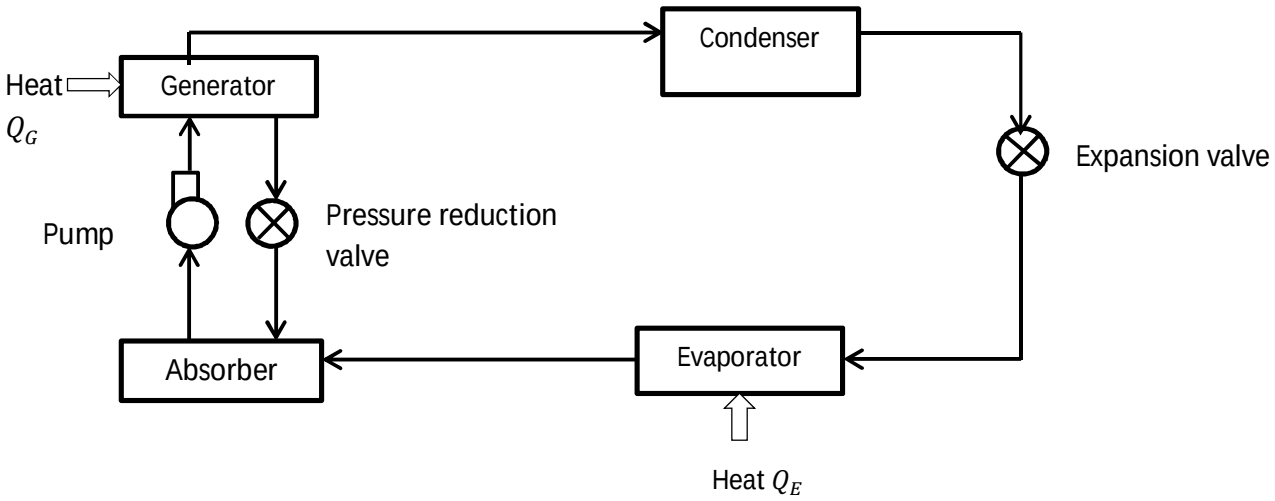

Fig. 3

Schematic of the heat recovery circuit:

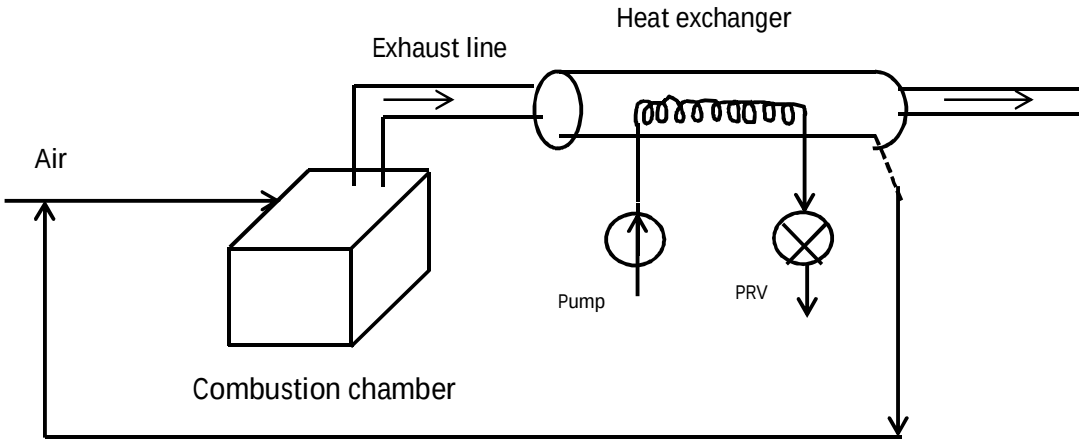

Fig. 4

The two fluids passing through the generator are exhaust gas and the absorbate refrigerant liquid. If liquid solution is made to flow through small channels then liquid velocity and Reynolds number will be higher. Therefore, Nu number will be higher and possibility of flow turbulence will be more. So the heat transfer coefficient will be higher and heat exchanger will be more compact.

In figure 4 a heat exchanger is placed on the exhaust gas flow path. An absorbate refrigerant liquid flows through the heat exchanger channels to capture waste heat. Also the outlet exhaust gas from the heat exchanger may be used to preheat the fresh air.

Refrigeration load calculation of the automobile engine

[Ref-CARRIER SYSTEM DESIGN HANDBOOK]

We consider an automobile with basic size:

Length-8 m*Breadth-2 m*Height-2 m

Glass area is assumed to be 50% of walls.

Solar heat gain,

$=[(8*2*2)*0.5+(2*2*2)*0.5]*10.76*12*0.5$ Btu/hour

$= 1291.2$ Btu/hour

Solar heat gain through wall,

$=[(8*2*2)*0.5+(2*2*2)*0.5]*10.76*26*0.3 = 1678.56$ Btu/hour

Transmission heat gain through glass,

$$= \text{area} * \Delta T_{\text{transmission}} * U_{\text{glass}}$$

$$= [(8*2*2)*0.5+(2*2*2)*0.5]*10.76*29*1.0$$

$$= 6240.8 \text{ Btu/hour}$$

Heat gain through roof,

=8*2*10.76*29*0.5=2496.32 Btu/hour

Heat gain through floor,

=8*2*10.76*29*0.5=2496.32 Btu/hour

Heat gain from people,

=50*700=35000 Btu/hour

Heat gain from equipments,

=Brake horsepower of the engine*bsfc*lower heating value of the fuel*% of heat gained*unit conversion

$$= 201.153\ \text{hp} * 0.2\ \frac{\text{Kg}}{\text{hp. hour}} * 43000\ \frac{\text{KJ}}{\text{Kg}} * 0.005 * \frac{3400}{3600}$$

$$= 8169.047\ \text{Btu/hour}$$

Ventilation air heat gain considering two air changes per hour,

$$= 8 * 2 * 2 * 10.76 * 3.28 * 2 * \frac{1}{60} * 29 * 1.08$$

$$= 1179.062\ \text{Btu/hour}$$

Latent heat gain,

Heat gain from people $= 50 * 500 = 25000\ \text{Btu/hour}$

Thus, total heat gain=total cooling load,

$$= 1291.2 + 1678.56 + 6240.8 + 2496.32 + 2496.32 + 35000 + 8169.047 + 1179.062 + 25000$$

$$= 83551.309\ \text{Btu/hour}$$

$$= \frac{83551.309}{12000} = 6.96261\ \text{tonne of refrigeration}$$

$$[\text{Since}, 12000\ \frac{\text{Btu}}{\text{hour}} = 1\text{TR} = 3.5\ \text{KW}\ ]$$

Then, the cooling load estimated for air-conditioning of the car,

$$\dot{Q}_l = 6.96261\ \text{TR} = 6.96261 * 3.5\ \text{KW} = 24.369\ \text{KW}$$

Calculation of the heat transfer required in the generator:

We consider the operation of a $H_2o - LiBr$ chilled water plant for air conditioning purpose. The general operating conditions are as follows- Generator temperature is 97 °C, Condenser temperature is 40 °C, Chilled H_2o temperature is 10 °C, and absorber temperature is 40 °C. For the 6.96261 tonne refrigeration capacity the following are to be calculated:

1. Thermodynamic states of all points
2. Coefficient of performance of the refrigeration plant
3. Mass flow rates from and to the parts of the refrigeration plant
4. And energy balance of whole the refrigeration system

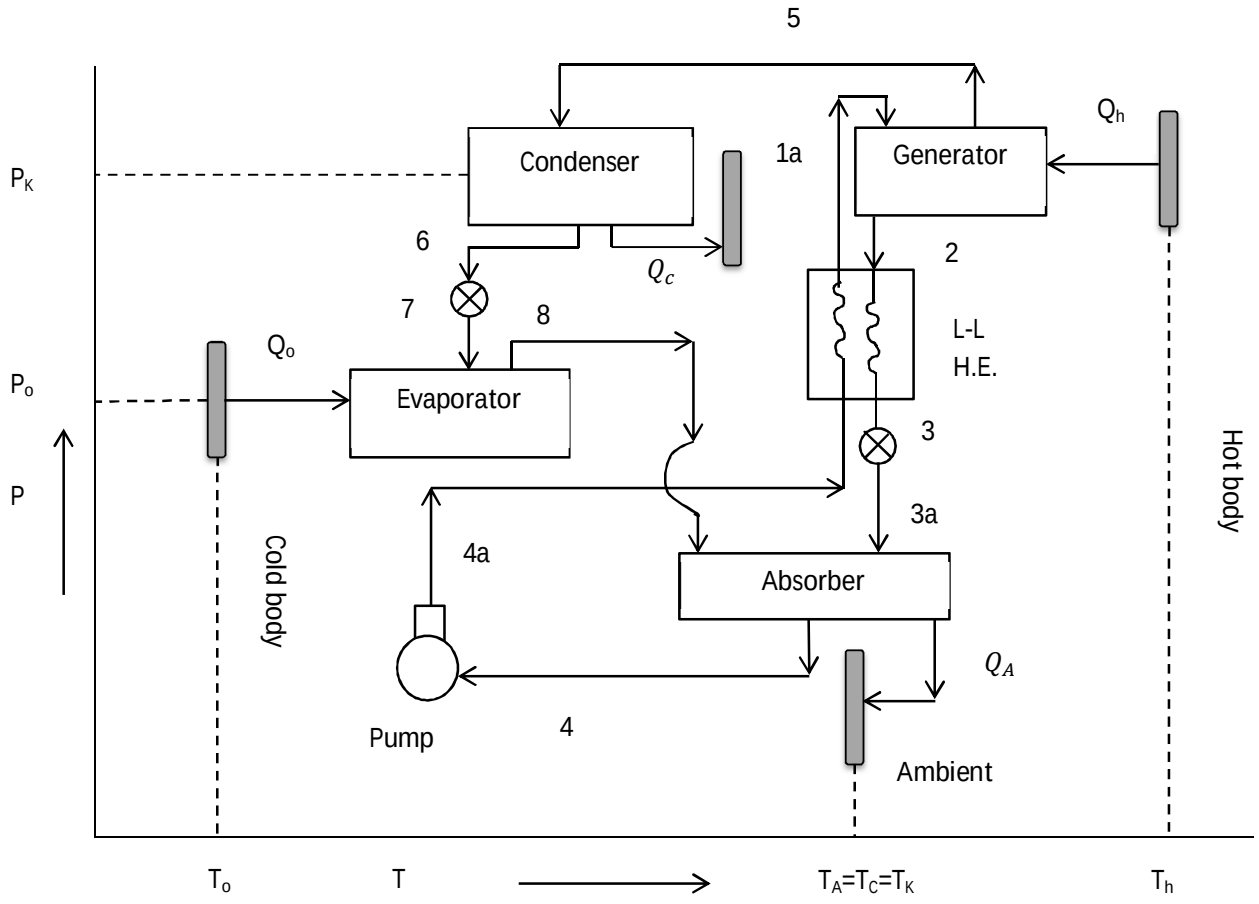

Fig 5. Schematic representation of the cooling circuit

From table of H_2O vapor pressure, the evaporator pressure and condenser pressure is obtained.

Condenser pressure = generator pressure = 55.32 mm of Hg (At 40 ℃)

Flash chamber and absorber pressure =9.21 mm of Hg (At 10 ℃)

The concentrations of LiBr and H_2O in the rich and weak solutions are obtained from ln P-1/T diagram at state 4 and 2.

State 4

Saturated cold solution from absorber at P=9.21 mm of Hg=1.228 KPa and $t_4 = 40$ ℃

$$\xi_r = 1 - \xi_{LiBr} = 1 - 0.55 = 0.45$$

State 2

Saturated hot solution from the generator at P=55.32 mm of Hg =7.375 KPa and t= 90 ℃

$\xi_{LiBr_2} = 0.65, h_2 = 248$KJ/Kg using h-$\xi_r$ diagram.

Poor solution concentration of H_2O is $\xi_a = 1 - 0.65 = 0.35$

State 1

Saturated solution at condenser pressure and 0.55 LiBr concentration:

T_1=74 ℃ from ln P-1/T diagram and h_1=166 KJ/Kg using h-ξ_r diagram

State 3

Saturated solution at evaporator pressure and 0.65 LiBr concentration

T_3=60 ℃ and h_3=180 KJ/Kg

State 3a

This state has the same enthalpy, temperature and composition as state 3.

But it is at the generator pressure. It is in a subcooled state from 2 to 3 at 55.32 mm Hg pressure.

State-4a

Point 4a after pumping is in subcooled state at 55.32 mm of Hg

T=40 ℃, ξ_{LiBr} = 0.55

h_{4a} = h_4 =93.5 KJ/Kg (neglecting pump work)

Specific solution circulation rates

$$f = \frac{1 - 0.35}{0.45 - 0.35} = 6.5 \text{ Kg/Kg vapor}$$

Or, f-1=5.5 Kg/Kg vapor

Heat available in the hot solution for transfer

$$=(f-1)(h_2-h_3)=5.5*(248-180)=374 \text{ KJ}$$

Heat required for the cold solution for heating

$$=f(h_1-h_4)=6.5*(166-93.5)=471 \text{ KJ}>374 \text{ KJ}$$

Thus the cold solution at 4a cannot be heated to 1.

From liquid to liquid heat exchanger's energy balance equation,

$$f * (h_{1a} - h_{4a}) = (f - 1)(h_2 - h_3)$$

Now h_{4a} = h_4 and $c_{p,l}$ = 1925 J/KgK

Or, $f * (t_{1a} - t_4) = \frac{(f-1)(h_2-h_3)}{c_{p,l}}$

$$Or, t_{1a} = \frac{5.5 * (248 - 180) * 1000}{1925 * 6.5} + 40 = 29.89 + 40 = 69.89 \text{ ℃}$$

$$h_{1a} = \frac{(f - 1)(h_2 - h_3)}{f} + h_{4a} = 151 \text{ KJ/Kg}$$

State-5

It represents the superheated state of water vapor at 55.32 mm of Hg pressure and 97 ℃ temperature. The enthalpy at this state can be calculated using the formula,

h=2501+1.88t KJ/Kg

Thus, h_5=2501+1.88*97=2683 KJ/Kg

State 6

It is the state of saturated water at 40 ℃

$$h_6 = c_{water} * 40 = 4.1868 * 40 = 167.5 \text{ KJ/Kg}$$

State 7

It is the Liquid +vapor state after throttling

P=9.21 mm of Hg and t=10 ℃

State 8

It is the saturated vapor state

P=9.21 mm of Hg and t=10 ℃

Refrigeration effect is calculated as follows,

$$q_0 = h_8 - h_7 = 2520 - 167.5 = 2352.5 \text{ KJ/Kg}$$

Heat added in the generator for 1 Kg of vapor distilled,

$$q_h = h_5 - h_2 + f * (h_2 - h_{1a}) = 2683 - 248 + 6.5 * (248 - 151)$$
$$= 3066 \text{ KJ/Kg of vapor}$$

Then, COP$\approx \frac{q_0}{q_h} = \frac{2352.5}{3066} = 0.77$

Water vapor distilled =D=$\frac{211*1}{2352.5}$ = 0.09 Kg/min per tonne of refrigeration

Mass flow rate of cold solution from the absorber=F=f*D=6.5*0.09=0.585 Kg/min per tonne of refrigeration.

Mass flow rate of hot solution from the generator=F-D=0.5-85-0.09=0.495 Kg/min per tonne of refrigeration.

Heat rejected in the condenser=$Q_c = \frac{D}{60} * (h_5 - h_6) = \frac{0.09*(2683-167.5)}{60}$

$Or, Q_c = 3.77\ KW$ per tonne of refrigeration.

Heat rejected in the absorber,

$$Q_A = D * q_A = D * [(h_8 - h_3) + f * (h_3 - h_4)]$$

$Or, Q_A = \frac{0.09}{60} * [(2520 - 180) + 6.5 * (180 - 93.5)] = 4.35$ KW per tonne of refrigeration.

Heat supplied in the generator $= Q_h = D * q_h = \frac{0.09}{60} * 3066 = 4.6\ KW$ per tonne of refrigeration.

Heat absorbed in evaporator $= Q_0 = 3.5167$KW per tonne of refrigeration.

Net heat received $= Q_h + Q_0 = 4.6 + 3.5167 = 8.12$ KW per tonne of refrigeration.

Net heat rejected $= Q_c + Q_A = 3.77 + 4.35 = 8.12$KW per tonne of refrigeration.

So, the energy balance matches closely.

Heat exchanger performance calculation

Now for an engine of rated power=150 KW,

$$\text{Engine's bsfc} = 0.2\ \frac{\text{kg}}{\text{bhp.hour}} = \frac{0.2}{0.7457}\ \frac{\text{Kg}}{\text{KW.hour}} = 0.2682\ \frac{\text{Kg}}{\text{KW.hour}}$$

$$= \frac{0.2682}{1000 * 3600}\ \text{Kg/W.Sec}$$

Now, $\frac{\dot{m}_f}{bp} = \text{bsfc}$

$$\text{Or, } \dot{m}_f = \text{mass flow rate of fuel} = \frac{0.2682 * 150 * 1000}{1000 * 3600}$$

$$\text{Or, } \dot{m}_f = 0.011175\ \text{kg/sec}$$

Diesel engine at full load operates at near 22:1 air fuel ratio.

$$\text{So, } \dot{m}_a = 22 * \dot{m}_f\ \text{kg/sec}$$

$$\dot{m}_{\text{exhaust gas available}} = \dot{m}_h = \dot{m}_a + \dot{m}_f = 23 * \dot{m}_f = 0.25703\ \text{kg/sec}$$

The specific heat of the exhaust gas,

$$c_{p,g} = 1.130\text{KJ/KgK}$$

It is assumed that the exhaust gas leaves the combustion chamber at temperature 450 ℃ (as per standard data). It is further assumed that due the heat extracted in the heat exchanger, exhaust gas temperature drops to 110 ℃ at the exit of the heat exchanger.

Then maximum heat available from the exhaust gas for extraction,

Q_{max}=0.25703*1.130*(450-110) K W = =98.751 KW

Then the heat that can actually be delivered to generator assuming a 60 % effectiveness of the heat exchanger,

=0.6*98.751 KW=59.25 KW

Then, refrigeration capacity at full load that can be achieved,

$$= \frac{59.25}{4.6}\ \text{TR} = 12.880\ \text{TR}$$

As the refrigeration load required=6.96261 TR, so refrigeration is possible.

$$\text{COP}_{\text{refrigeration}} = 0.77 = \frac{\dot{Q}_l}{\dot{Q}_g} = \frac{24.369\ \text{KW}}{\dot{Q}_g}$$

$$\dot{Q}_g = \frac{24.369}{0.77} = 31.648\ \text{KW}$$

$$\dot{m}_g = \text{actual exhaust gas flow} = \frac{31.648 * 1000}{1130 * (450 - 110)}$$

Or, $\dot{m}_g = 0.08237\ \text{kg/sec}$

The remaining exhaust gas is to be bypassed.

$$D = \frac{211 * 6.96261}{2352.5}\frac{\text{Kg}}{\text{min}} = 0.6245\ \frac{\text{Kg}}{\text{min}}$$

F = mass flow rate of strong cold solution from the absorber $= \dot{m}_l = f * D$

$$= 6.5 * 0.6245 = 4.0592\ \frac{\text{Kg}}{\text{min}}$$

$\dot{m}_l = 0.06765\ \text{Kg/sec}$

Design using plate fin heat exchanger

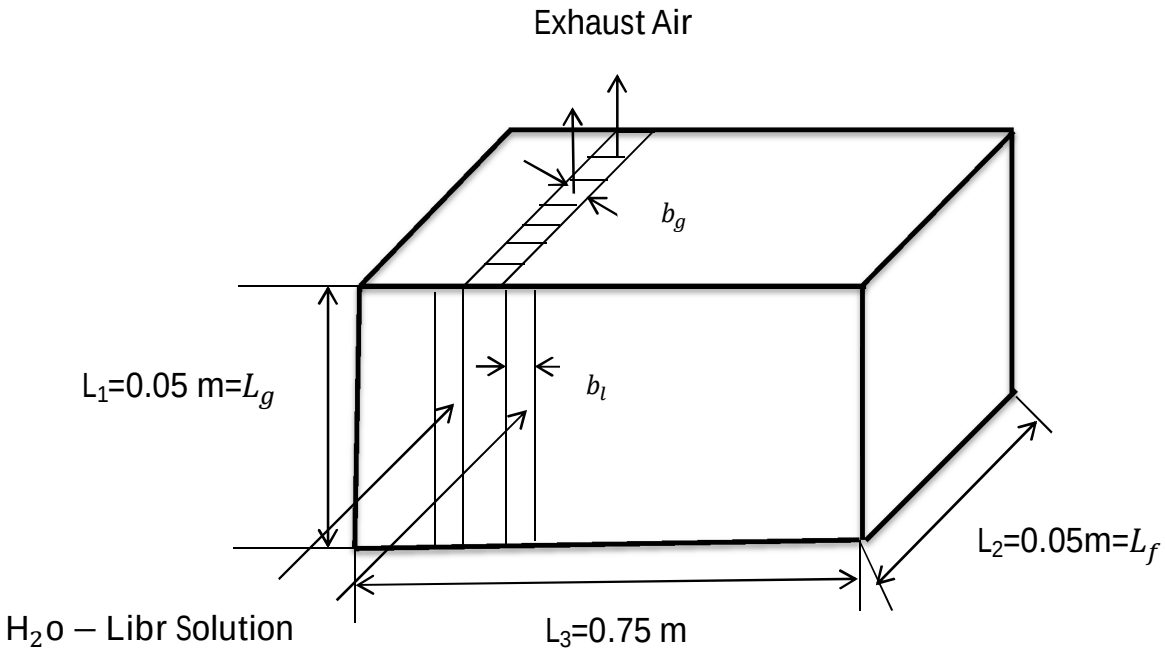

Fig 6. Plate fin heat exchanger schematic

Let the number of passes of hot heat exchanger gas be N_p

Then, H_2O-LiBr liquid should have N_p+1 number of passes to minimize heat loss to ambient from hot fluid passes.

Now, $L_3 = N_p * b_g + (N_p + 1) * b_l + (2 * N_p + 1)\delta_w$

Where, δ_w = wall thickness or plate thickness

b_g = plate spacing in exhaust gas passes

and b_l = plate spacing in liquid passes

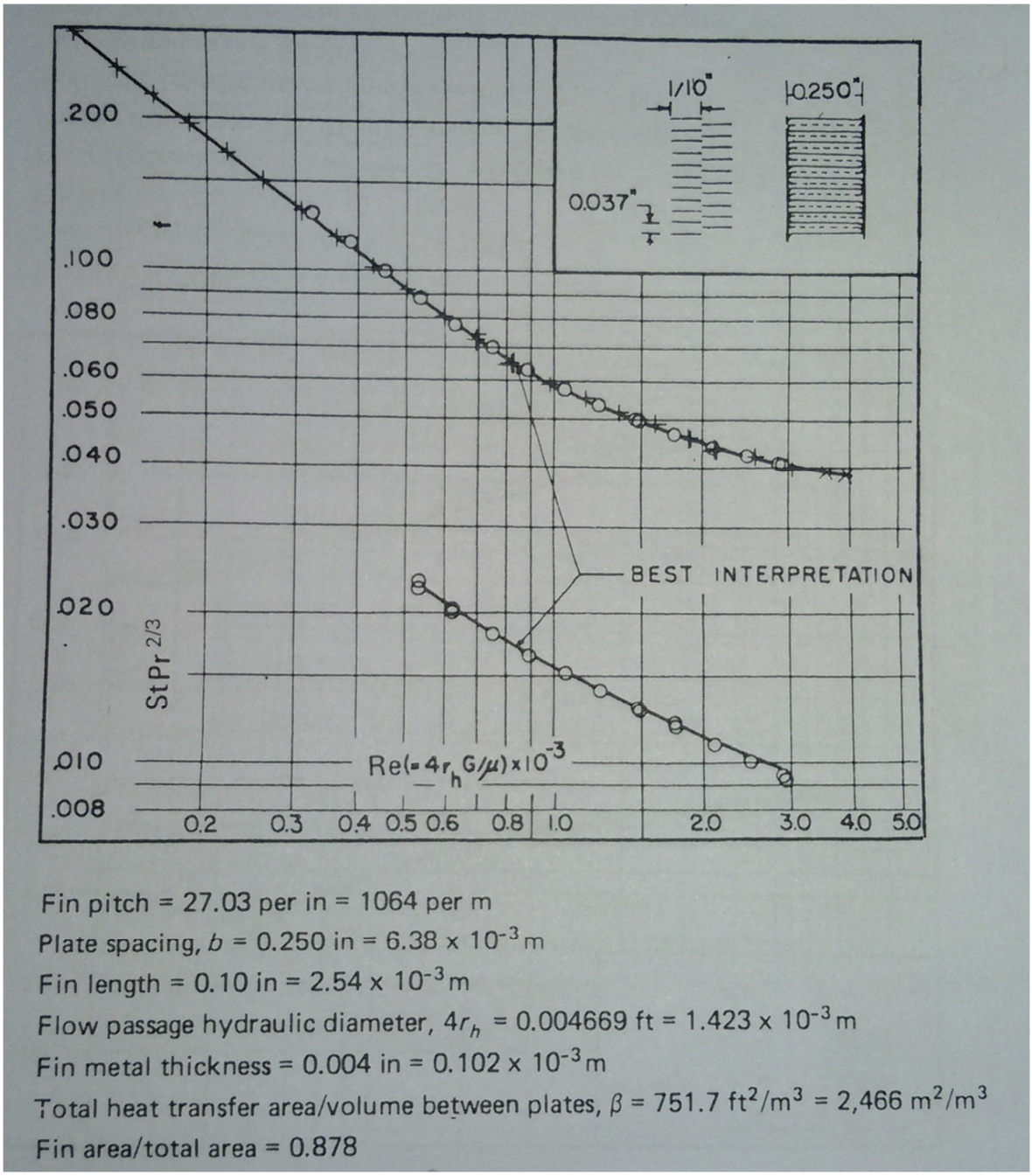

Fig 7. Strip fin plate fin surface used in the exhaust gas side

So,

$$N_p = \frac{L_3 - b_l + 2 * \delta_w}{b_g + b_l + 2 * \delta_w} = \frac{0.75 - 6.35 * 10^{-3} + 2 * 0.5 * 10^{-3}}{6.38 * 10^{-3} + 6.35 * 10^{-3} + 2 * 05 * 10^{-3}}$$

$$N_p = 54.235$$

So, $N_p = 55$ taken

$A_{fr,g} = L_2 * L_3 = 0.05 * 0.75 = 0.0375\ m^2$

The heat exchanger volume between plates, on gas side are,

$V_{p,g} = L_1 * L_2 * b_g * N_p = 0.05 * 0.05 * 6.38 * 10^{-3} * 55 = 0.00087725\ m^3$

Heat transfer area of gas side is,

$A_g = \beta_g * V_{p,g} = 2.1632985\ m^2$

Heat transfer area in H_2O-LiBr solution side is,

$A_l = L_1 * L_2 * 2 * N_p = 0.275\ m^2$

The minimum flow area of gas side is,

$$A_{o,g} = \frac{D_{h,g} * A_g}{4 * L_g} = 0.015392\ m^2$$

Then, the ratio of minimum free flow area to frontal area in gas side,

$$\sigma_g = \frac{A_{o,g}}{A_{fr,g}} = 0.411$$

Then,

$$G_g = \frac{\dot{m}_g}{A_{o,g}} = 5.35148\ Kg/m^2sec$$

Then,

$$Re_g = \frac{G_g * D_{h,g}}{\mu_g} = 273.926$$

From Kays and London[53], For the above fluids, by suitable extrapolation,

$$St_g . Pr_g^{\frac{2}{3}} = 0.0301 = j_g \text{ and } f_g = 0.1485$$

The heat transfer coefficients are calculated to be,

$$h_g = \left[\frac{j * G * c_p}{Pr^{2/3}}\right]_g = 221.256$$

Now the fin parameters are defined as ,

$$m_g = \left[\frac{2 * h_g}{k_{f,g}\delta_g}\left(1 + \frac{\delta_g}{l_{s,g}}\right)\right]^{1/2}$$

$k_{f,g}$ is thermal conductivity of the fin material in the gas side

Here, Inconel fin is used, so, $k_{f,g} = 16.05 W/mK$

So,

$$m_g = \left[\frac{2 * 221.256}{16.05 * 0.102 * 10^{-3}} * (1 + \frac{0.102 * 10^{-3}}{2.54 * 10^{-3}})\right]^{1/2} = 530.24$$

$$A_{o,l} = (N_p + 1) * L_1 * L_2 = 56 * 0.05 * 0.05 = 0.14\ m^2$$

$$G_l = \frac{\dot{m}_l}{A_{o,l}} = \frac{0.06765}{0.14} = 0.4832\ Kg/m^2 sec$$

Now,

$T_{ci} = t_4 + 29.89℃ = 69.89\ ℃$ and $T_{co} = 90℃$

So,

bulk mean temperature of the $H_2O - LiBr$ solution $= \frac{69.89+90}{2} = 79.945\ ℃$

Where, c_{pl} = specific heat of $H_2o - LiBr$ solution

$$So, c_{pl} = \frac{c_{pl,i} + c_{pl,o}}{2} = \frac{c_{p,l}{}_{\xi=0.55} + c_{p,l}{}_{\xi=0.65}}{2} = \frac{2.05 + 1.8}{2} = 1.925\ KJ/KgK$$

k_l = 0.668 at the H_2o Libr solutions bulk mean temperature 79.945 ℃

Now,

$$\mu_{l@79.945\,℃} = 2.7 * 10^{-3}\ \text{Pa.s}$$

In the liquid side there is internal forced convection flow through the duct.

Cross sectional area of the duct = $A_c = 0.05 * 6.35 * 10^{-3}$

Or, $A_c = 317.5 * 10^{-6}\ m^2$

P = perimeter of the duct = $2 * (6.35 * 10^{-3} + 0.05)$ m = 0.1127 m

So,

$$D_{h,l} = \frac{4 * A_c}{P} = \frac{4 * 317.5 * 10^{-6}}{0.1127} = 11.269 * 10^{-3}\ m$$

$$Pr_g = \frac{\mu_g c_{p,g}}{k_g} = \frac{27.8 * 10^{-6} * 1.130 * 10^3}{0.0421}$$

$Pr_g = 0.746$

$$Pr_l = \frac{\mu_l c_{p,l}}{k_l} = \frac{0.00335 * 1925}{0.668}$$

$Pr_l = 7.780689$

$$Re_l = \frac{G_l * D_{h,l}}{\mu_l} = \frac{0.4832 * 11.269 * 10^{-3}}{2.7 * 10^{-3}} = 2.0167$$

For constant surface temperature in duct flow[54],

$$\text{For } a/b = \frac{0.05}{6.35 * 10^{-3}} = 7.874$$

,

$$Nu = 5.57 = \frac{h_l D_{h,l}}{k_l}$$

$$\text{Or,}\quad h_l = \frac{5.57 * 0.668}{11.269 * 10^{-3}} = 330.176\ \text{W/m}^2\text{K}$$

$$\text{And,}\qquad f_l = \frac{82.32}{\text{Re}} = 2.9516$$

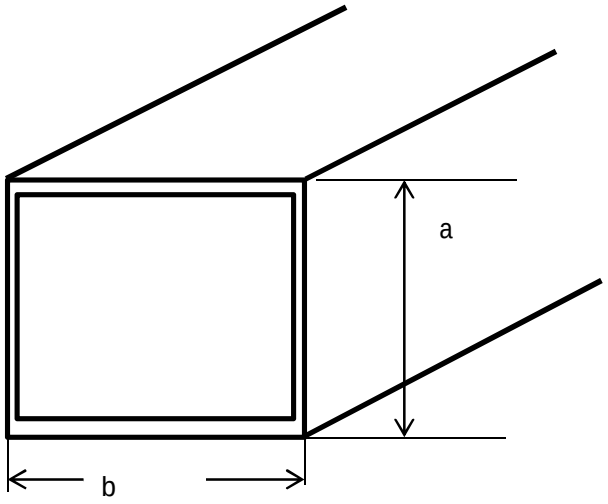

Fig 8. Duct flow

Fin efficiency for gas side is,

$$\eta_{f,g} = \frac{\tanh m_g l_g}{m_g l_g}$$

Where l_g and l_l are fin lengths for heat conduction.

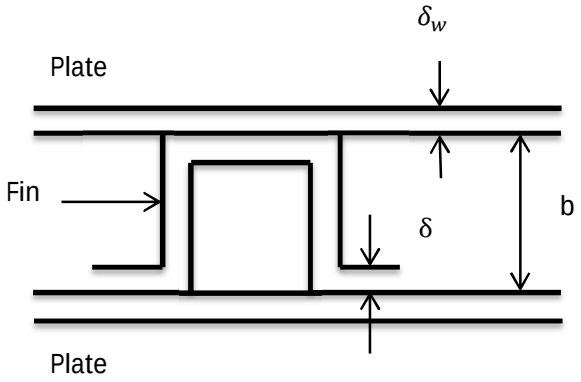

Fig 9. Offset strip fin

$$l_g = \frac{b_g}{2} - \delta_g = \frac{6.38 * 10^{-3}}{2} - 0.102 * 10^{-3}$$

$$l_g = 3.088 * 10^{-3}$$

$$\eta_{f,g} = \frac{\tanh(530.24 * 3.088 * 10^{-3})}{530.24 * 3.088 * 10^{-3}} = 0.5662$$

Then the overall surface efficiencies are,

$$\eta_{o,g} = \left[1 - (1 - \eta_f)\left(\frac{A_f}{A}\right)\right]_g = [1 - (1 - 0.5662) * 0.878] = 0.6191$$

$$\text{As,} \qquad \left(\frac{A_f}{A}\right)_g = 0.878$$

Wall resistance is calculated as follows,

$$A_w = L_1 L_2 (2 * N_p + 2) = 0.05 * 0.05 * (2 * 55 + 2) = 0.28\ m^2$$

$$R_w = \frac{\delta_w}{k_w A_w} = \frac{0.5 * 10^{-3}}{0.28 * 16.05} = 111.259 * 10^{-6}\ K/W$$

$$\frac{1}{UA} = \frac{1}{(\eta_0 hA)_g} + \frac{1}{(hA)_l} + R_w$$

$$\text{Or,} \quad \frac{1}{UA} = \frac{1}{0.9504 * 221.256 * 2.1632985} + 111.259 * 10^{-6} + \frac{1}{330.176 * 0.275}$$

$$\frac{1}{UA} = 2.198275 * 10^{-3} + 111.259 * 10^{-6} + 11.0134 * 10^{-3}$$

$$\frac{1}{UA} = 0.01332 \text{ or, } UA = 75.058$$

Heat capacity rates,

$$C_g = \dot{m}_g c_{p,g} = 0.08237 * 1130 = 93.078$$

$$C_l = \dot{m}_l c_{p,l} = 0.06765 * 1925 = 130.23$$

$$Or, C_{min} = C_g = 93.078$$

$$So, NTU = \frac{UA}{C_{min}} = \frac{75.058}{93.078} = 0.806$$

$$And, C^* = \frac{C_{min}}{C_{max}} = \frac{93.078}{130.23} = 0.715$$

For these values of NTU and C^*, the effectiveness of the heat exchanger is found out. For a crossflow heat exchnger, one fluid mixed and the other one unmixed,

The expression of effectiveness is,

$$\varepsilon = 1 - \exp[-\frac{\{1 - \exp(-NTU * C^*)\}}{C^*}]$$

$$\varepsilon = 45.81\ \%(approx)$$

So, this efficiency is very low and also does not match the minimum efficiency of the heat exchanger that was assumed. Then, the heat exchanger area is increased by using a second block of the heat exchanger above it.

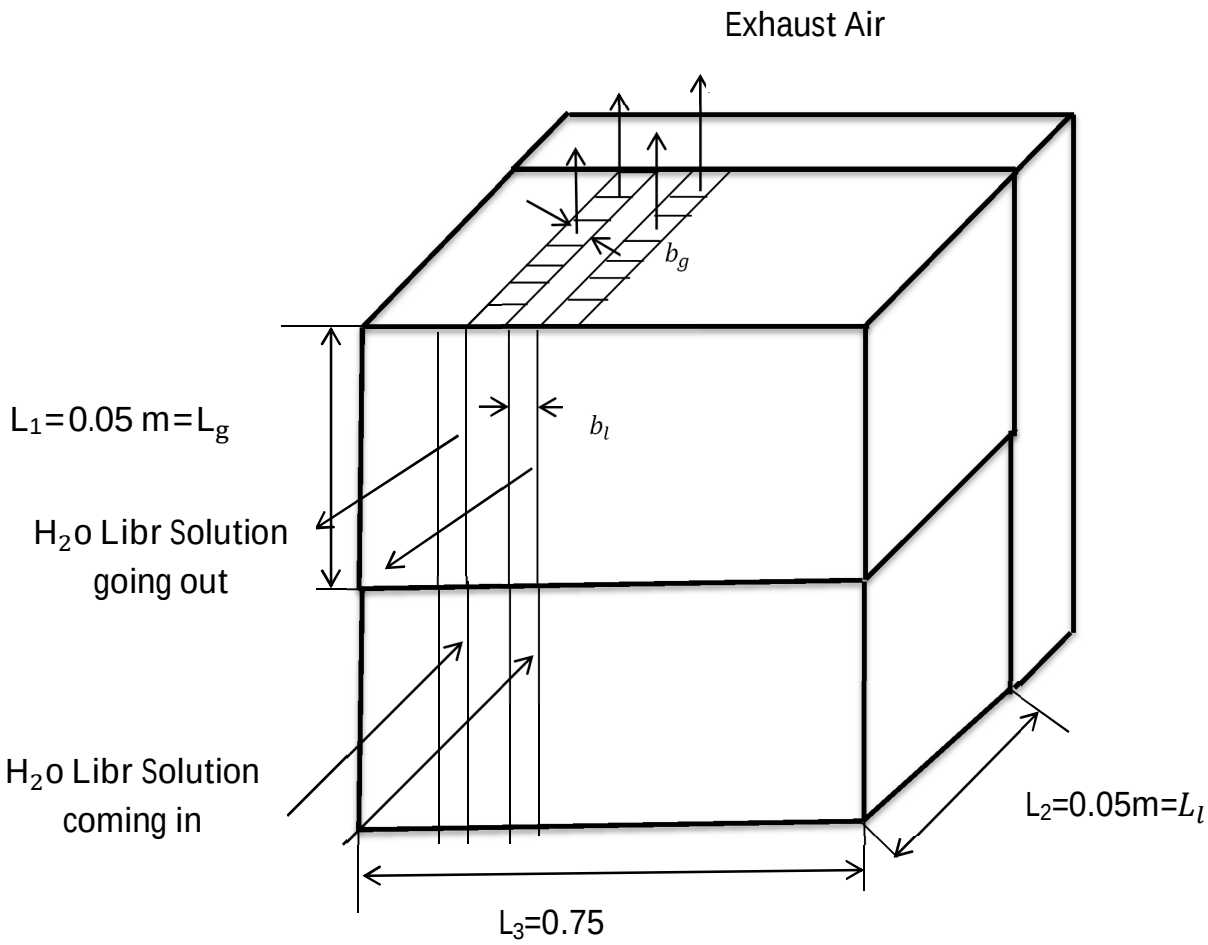

Fig 10. Heat exchanger schematic

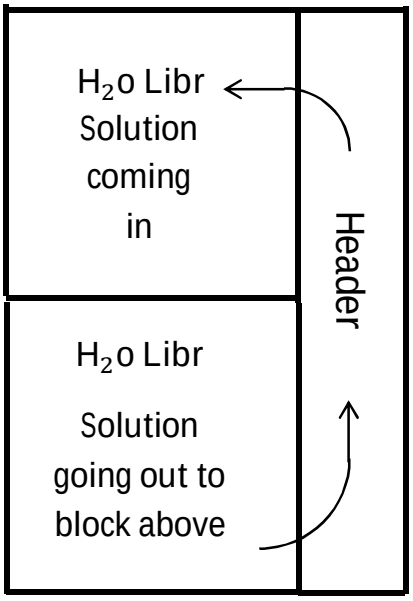

Fig 11. side view of the heat exchanger

$$\text{So, NTU} = \frac{UA}{C_{min}} = \frac{150.116}{93.078} = 1.6128$$

$$\text{And, } C^* = \frac{C_{min}}{C_{max}} = \frac{93.078}{130.23} = 0.715$$

For these values of NTU and C^*, the effectiveness of the heat exchanger is found out,

For a crossflow, one fluid mixed and the other one unmixed,

The expression of effectiveness is,

$$\varepsilon = 1 - \exp[-\frac{\{1 - \exp(-\text{NTU} * C^*)\}}{C^*}]$$

$$\varepsilon = 61.6\ \%$$

Thus, ε is approximately the same as the value assumed.

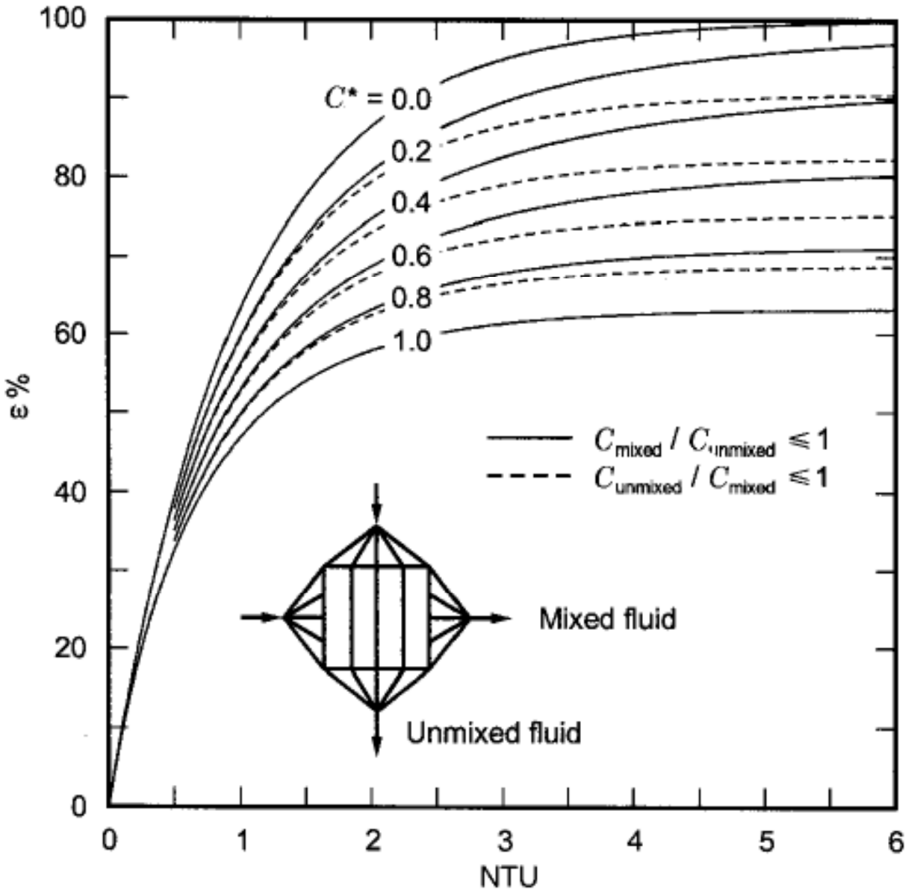

Fig 12. Effectiveness of a unmixed–mixed crossflow heat exchanger as a function of NTU and C*[52].

Pressure drops for the fluid flows are calculated as follows,

$$\Delta p_g = \frac{G_g^2}{2 * \rho_{g,i}} \left[(1 - \sigma^2 + K_c) + 2 * \left(\frac{\rho_i}{\rho_o} - 1 \right) + f * \frac{L * \rho_i}{r_h} * \left(\frac{1}{\rho} \right)_m - (1 - \sigma^2 - K_e) * \left(\frac{\rho_i}{\rho_o} \right) \right]_g$$

L here denotes the fluid flow path. So, fluid flow path for gas=L_g

Because of frequent boundary layer interruption in the offset strip fins, the gas and liquid flows are both very well mixed. The flows can be treated as if the Reynold's number is very high (Re $\rightarrow \infty$).

$$K_{c,g} = 0.34 \text{ and } K_{e,g} = 0.34$$

$$\Delta p_g = \frac{5.35148^{\,2}}{2 * 0.6158} * [1 - 0.411^2 + 0.34 + 2 * \left(\frac{0.6158}{0.7459} - 1\right) + \frac{0.1485 * 0.05 * 4 * 0.6158 * 1.4823}{1.423 * 10^{-3}} - (1 - 0.411^2 - 0.34) * \frac{0.6158}{0.7459}]$$

$$\text{Or}, \Delta p_g = 23.253 * (1.17108 - 0.3488 + 19.0514 - 0.4054)$$

As,

$$\left(\frac{1}{\rho}\right)_{m,g} = \frac{1}{2} * \left(\frac{1}{\rho_{g,i}} + \frac{1}{\rho_{g,o}}\right) = \frac{1}{2} * \left(\frac{1}{0.6158} + \frac{1}{0.7459}\right) = 1.4823$$

$$\Delta p_g = 452.7 \text{ Pa}$$

$$\Delta p_l = \frac{f_l * L_l * G_l^{\,2}}{2 * D_{h,l} * \rho_l} = \frac{2.9516 * 0.05 * 0.4832^2}{2 * 11.269 * 10^{-3} * 1250} = 0.00122 \text{ Pa}$$

As, the H_2O-LiBr liquid density is $\rho_{l,i} \cong \rho_{l,o} = \rho_l = 1250 \text{ kg/m}^3$

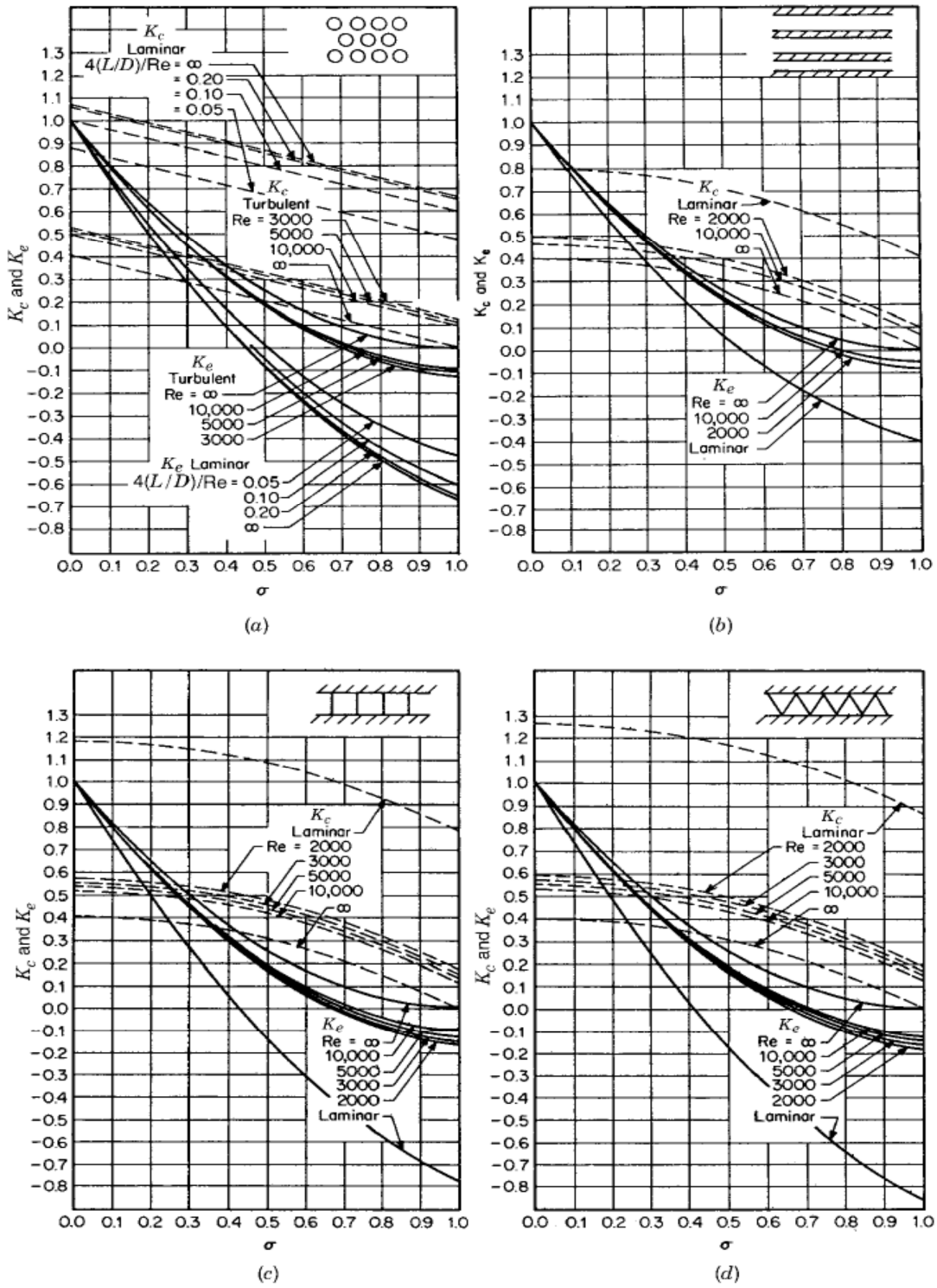

Fig 13. Entrance and exit pressure loss coefficients for (a) a multiple circular tube core, (b) multiple tube flat-tube core, (c) multiple square tube core, and d. multiple triangular tube core with abrupt contraction (entrance) and abrupt expansion (exit) [53]

Result

Load(KW)	total exhaust gas flow rate	m_g	C_g	C_l	NTU	c *	ε	Q_{max}	Q_g	Q_l
150	0.25703	0.0823699	93.078	130.23	1.6128	0.715	61.6	98.751	31.648	6.96261
140	0.2562	0.0745841	84.28	130.23	1.6128	0.647	63.26	107.55	31.648	6.96261
125	0.2551	0.0865487	97.8	130.23	1.6128	0.751	60.74	93.282	31.648	6.96261
110	0.254	0.0997434	112.71	130.23	1.6128	0.865	58.09	80.59	31.648	6.96261
100	0.2533	0.1112301	125.69	130.23	1.6128	0.965	55.85	72.072	31.648	6.96261
85	0.2521	0.1427434	161.3	130.23	1.6128	0.807	59.42	58.741	31.648	6.96261

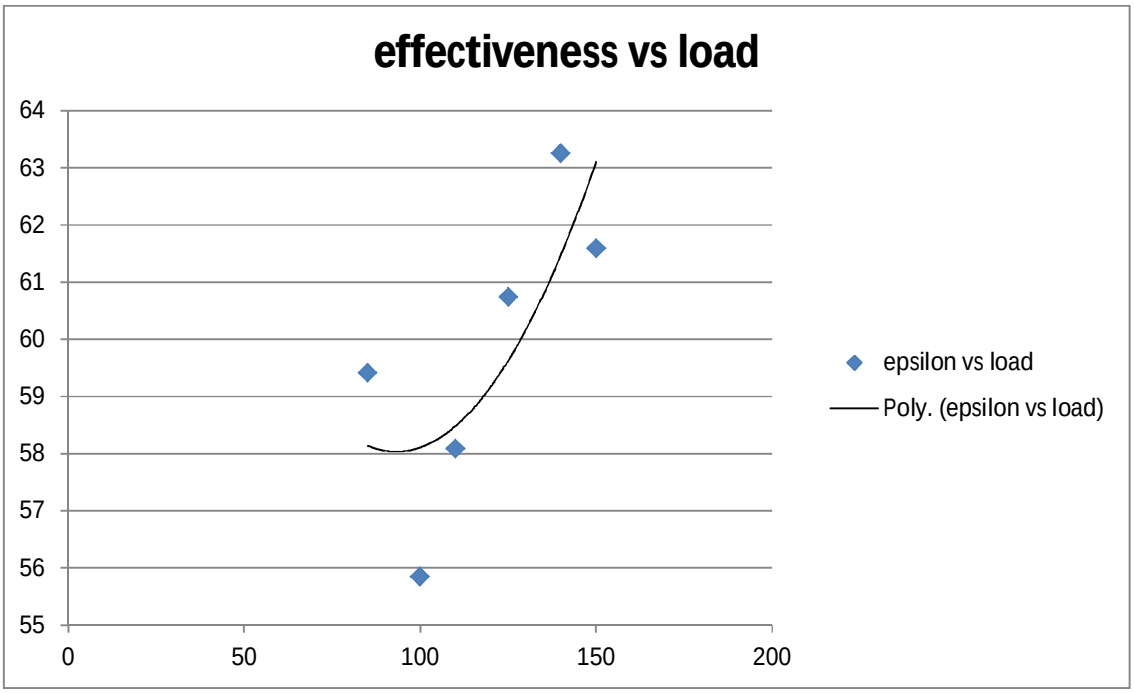

ϵ

Load (KW)

Fig 14.

Figure number 14 clearly indicate that with increase in load, the effectiveness of the heat exchanger at first decreases and then starts increasing after a certain value of load. This is because as the load increases, the exhaust gas temperature increases so available heat for extraction increases but at the same time the lost heat also increases. At lower loads the lost heat increases at higher rate than the former. So, effectiveness reduces with load increase at lower load. However, at higher load the effect of the first one is more compared to the second effect. Thus at higher load, as load increases, the effectiveness increases.

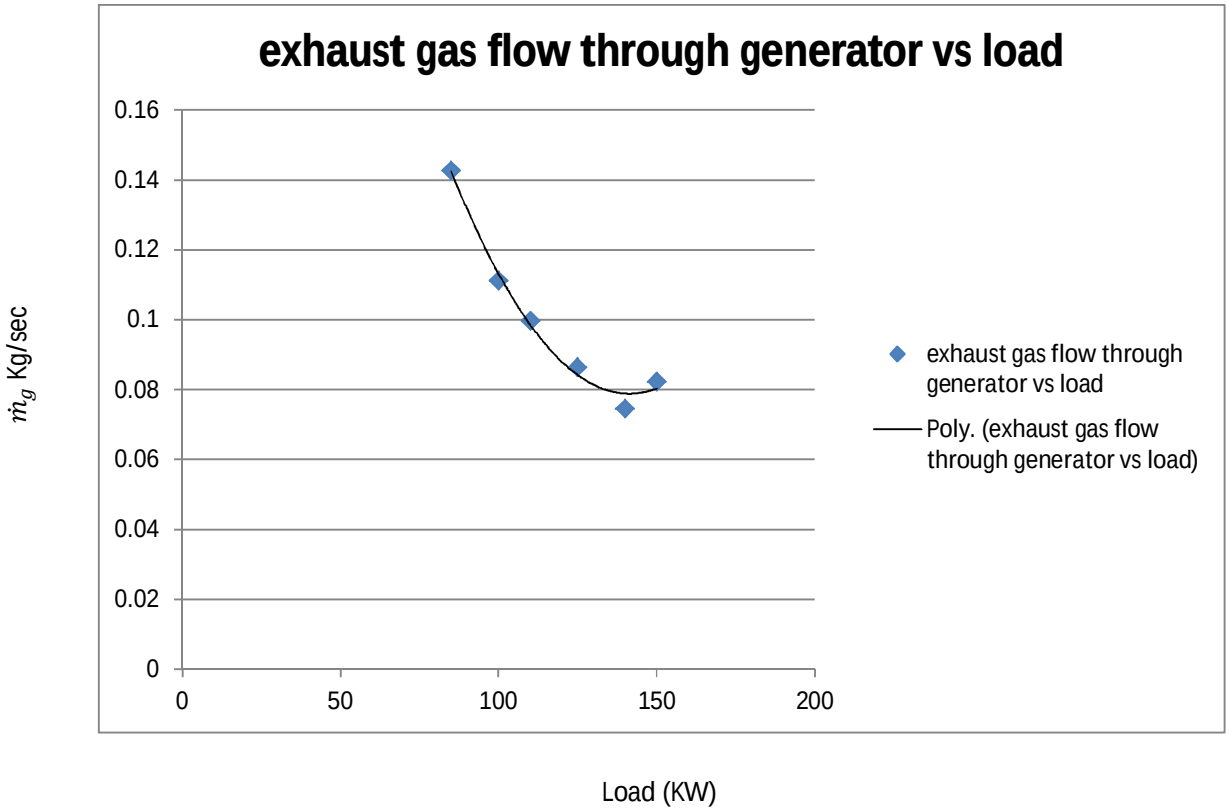

Fig 15

Figure number 15 clearly shows that as load increases the exhaust gas mass flow through the generator heat exchanger reduces. This is due to that fact that as load increases the heat contained in the same amount of exhaust gas increases. At higher loads, as the heat required to run the vapor absorption refrigeration system can be obtained from only a part of the exhaust gas, the remaining part of the exhaust gas flow is bypassed.

As load is reduced the heat contained in the exhaust gas reduces. So increasing amount of exhaust gas has to be passed through the generator heat exchanger to extract required amount of heat to run the vapor absorption refrigeration system.

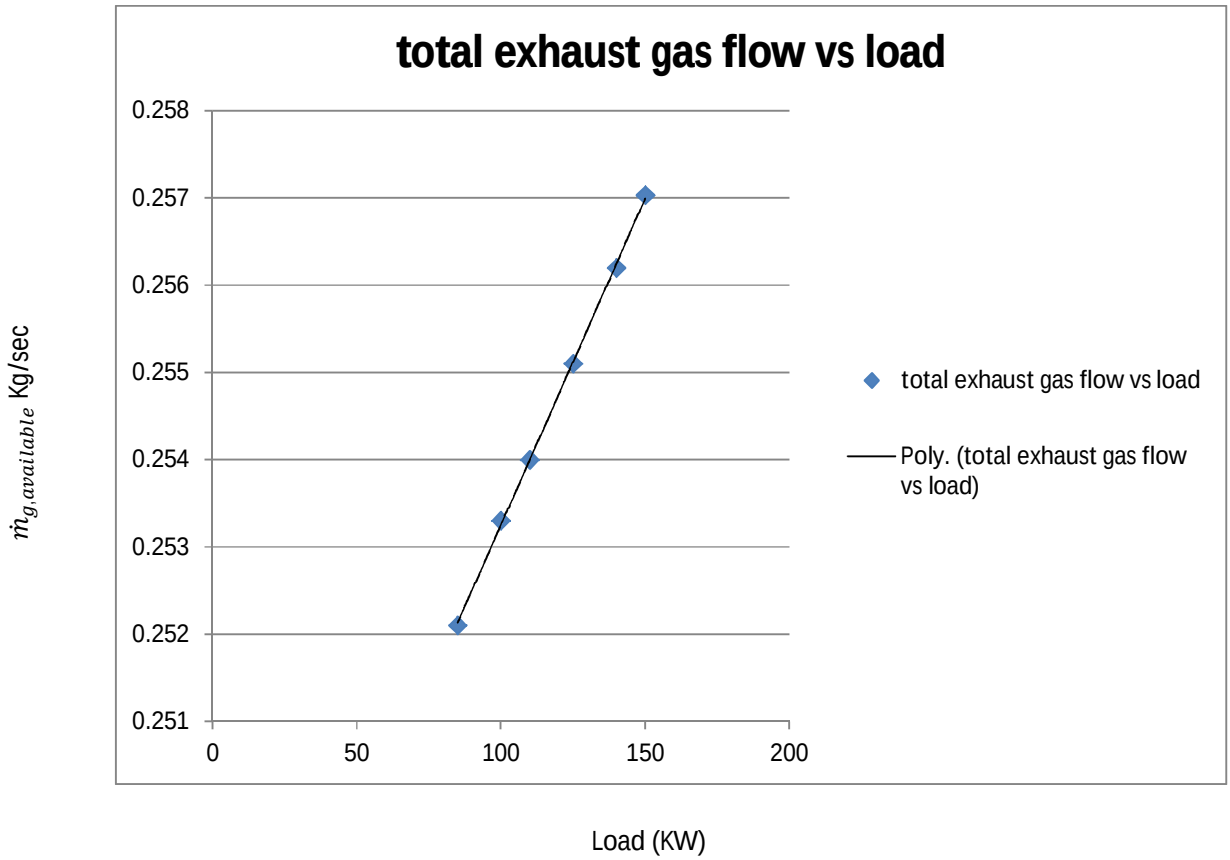

Fig 16

Figure number 16 shows that as load increases, the total exhaust gas mass flow increases. This is because in the diesel engine the air quantity is constant. The exhaust gas flow is the summation of the air and fuel mass flow rate. So, if mass flow of the fuel increases the exhaust gas flow increases. But the mass flow rate of the fuel is proportionate with the engine power. So, as engine power increases, the total exhaust gas mass flow rate also increases.

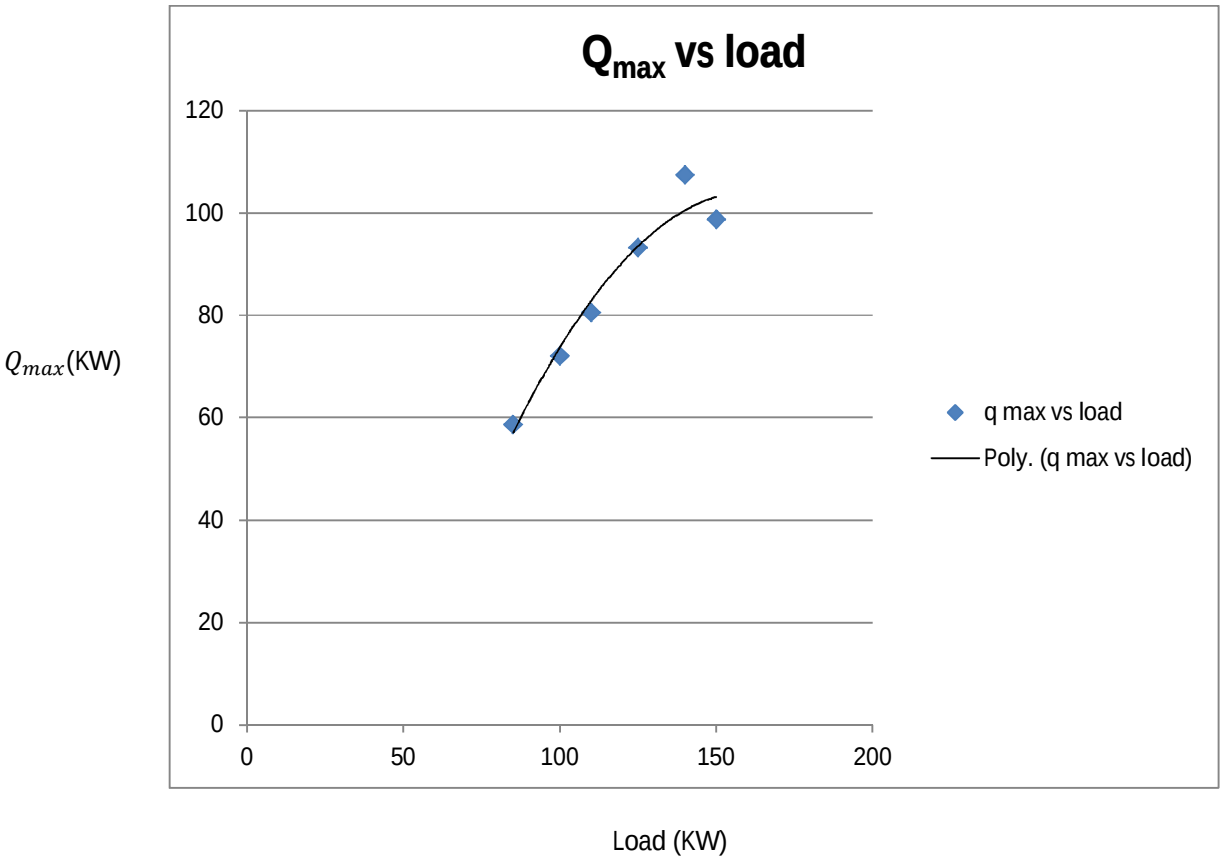

Fig 17

Figure number 17 shows that as load increases, the heat that can be extracted from the exhaust gas flow increases. This is because as load increases, the temperature of the exhaust gas increases as well as the mass flow rate of the exhaust gas. This combined effect results in higher heat content in the exhaust gas. However, at close to the rated power of the engine as the thermodynamic efficiency of the Diesel cycle becomes high, the rate of increase of exhaust heat content with load increase reduces to some extent. This flattens the curve near the full power.

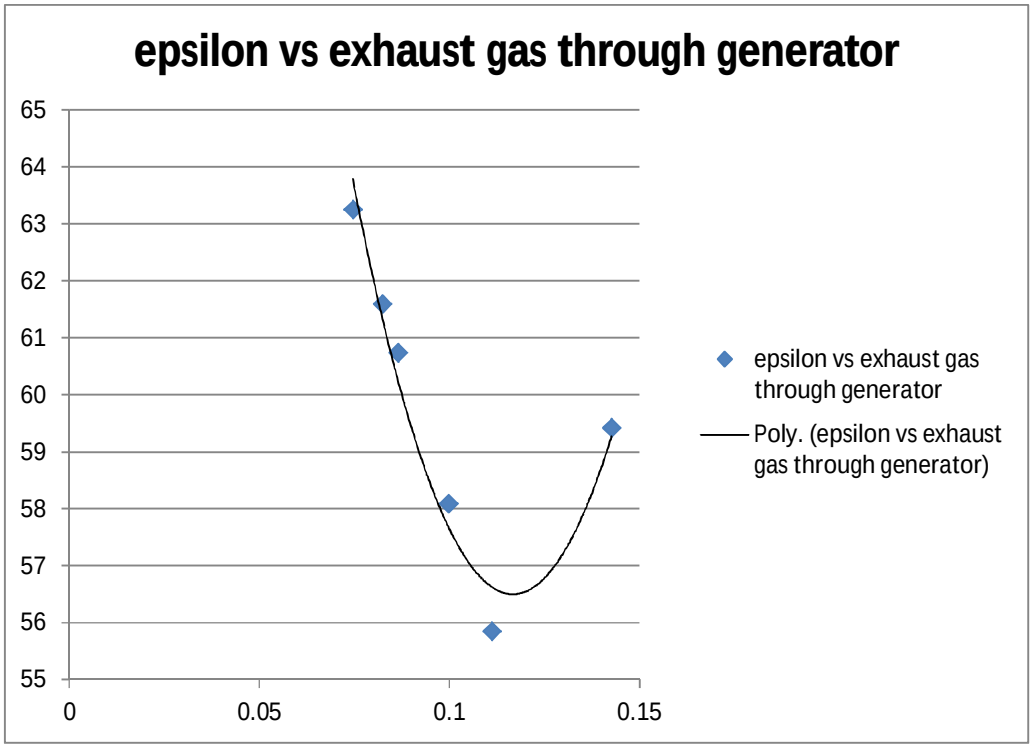

ϵ

$\dot{m}_g$ Kg/sec

Fig 18

Figure number 18 clearly shows that as the exhaust gas flow through the generator increases, the effectiveness of the heat exchanger at first reduces and then starts increasing after a certain load. This is because the higher amount of exhaust gas flows through the heat exchanger when the heat content of the exhaust gas is low. At this condition, which happens in low load, the exhaust heat energy is of low quality and less utilized by the heat exchanger. As the load increases, the heat content of the exhaust gas becomes more and less mass of exhaust gas flows through the generator. In both cases the heat exchanger extracts the same amount of heat. However, the higher temperature heat energy is better utilized by the heat exchanger as it is of higher quality and of higher exergy value.

Design using plate heat exchanger

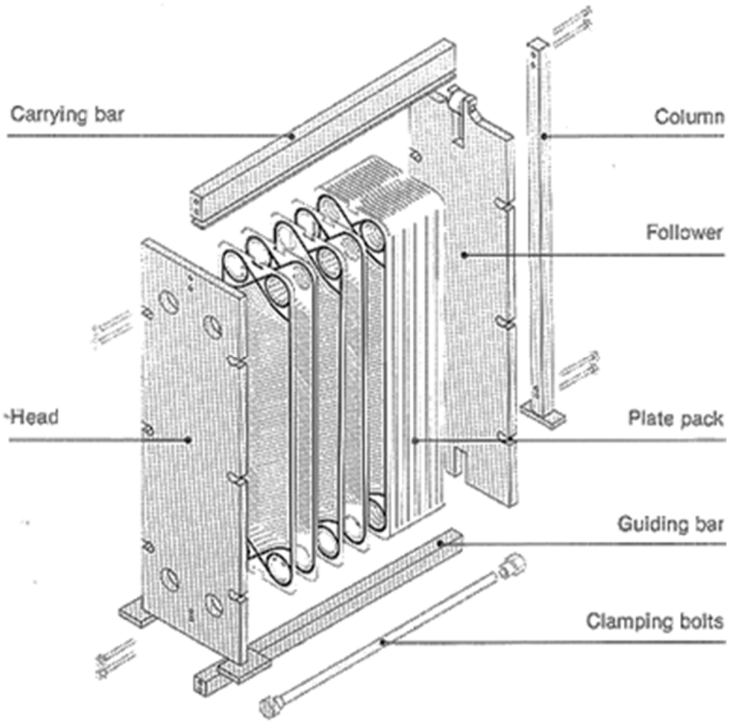

Fig 19. A gasketed plate heat exchanger

Exhaust gas inlet temperature $T_{g,i}$ = 450 ℃

Assuming approach of temperature at outlet as approximately 14 ℃,
$T_{g,o}$ = 84 ℃

Bulk mean temperature of exhaust gas =

$$\frac{T_{g,i} + T_{g,o}}{2} = \frac{450 + 84}{2} = 267\ ℃ = 540\ K$$

The properties of hot water are calculated at bulk mean temperature as follows,

$$\mu_g = \mu_{@267\ ℃} = 287.95 * 10^{-3}\ Pa.s$$

$$c_{p,g} = 1130\ J/KgK$$

$$\rho_g = \rho_{@267\ ℃} = 0.6384\ kg/m^3$$

$$k_g = k_{@267\ ℃} = 0.0438\ W/mK$$

On the other side of the heat exchanger the H_2O-LiBr solution will be passed which will take the heat from the exhaust gas.

$$LMTD = \Delta T_m = \frac{\Delta t_1 - \Delta t_2}{ln\frac{\Delta t_1}{\Delta t_2}} = \frac{(T_{g,i} - T_{l,o}) - (T_{g,o} - T_{l,i})}{ln\frac{(T_{g,i} - T_{l,o})}{(T_{g,o} - T_{l,i})}}$$

$$Or, \qquad \Delta T_m = \frac{(450 - 90) - (84 - 69.89)}{ln\frac{(450 - 90)}{(84 - 69.89)}} = \frac{360 - 14.11}{\ln\left(\frac{360}{14.11}\right)} = \frac{345.89}{3.2392}$$

$$Or, \qquad \Delta T_m = 106.78\ ℃$$

An overall heat transfer coefficient value is assumed,

$$U_O = 100\ \text{W/m}^2\text{K}$$

The overall area requirement is calculated as follows,

$$Q_l = 6.96261\ tonne = 24.369\ \text{KW}$$

$$\text{So, } A = \frac{Q_l}{U_O * \Delta T_m} = \frac{24.369 * 10^3}{100 * 106.78} = 2.2822\ m^2$$

Using the mechanical data for the heat exchanger plate,

Area per plate=0.96 m^2

$$\text{So, number of plate required} = \frac{2.2822}{0.96} = 2.378$$

So, we take 3 plates. Then, each fluid will have 1 channel with effective heat transfer area=$2 * 0.96\ m^2 = 1.92\ m^2$

$$\text{Then, } U_O = \frac{24.369 * 10^3}{1.92 * 106.78} = 118.86\ \text{W/m}^2\text{K}$$

The actual overall heat transfer is calculated as follows,

$$\frac{1}{U_c} = \frac{1}{h_g} + \frac{1}{h_l} + \frac{X_{wall}}{k_{wall}}$$

Where, h_g and h_l are the heat transfer coefficients in the exhaust gas side and H_2O-LiBr solution side respectively.

X_{wall} is the plate thickness and k_{wall} is the thermal conductivity of the plate.

Hot side calculation:

In ideal condition,

$$Re = \frac{\rho * v * D_h}{\mu}$$

However, the Reynold's number in plate heat exchanger is calculated using a plate specific empirical formula, Reynolds's number for plate heat exchanger,

$$Re = \frac{C_{Re} * \dot{M}}{\mu}$$

C_{Re} is a plate specific empirical constant for a channel, $\dot{M}$ is the mass flow per channel, and μ is the viscosity of the fluid.

$C_{Re} = 3063.6 * 10^{-3}$ from manufacturer's table

$$\dot{M}_g = \frac{0.08237}{1} = 0.08237 \text{ Kg/s per channel}$$

So,

$$Re_g = \frac{C_{Re} * \dot{M}_g}{\mu_g} == \frac{3063.6 * 10^{-3} * 0.08237}{287.95 * 10^{-3}} = 0.8764$$

Thus the flow is laminar. In that case,

$$Nu_g = 0.51008 {Re_g}^{0.333} {Pr_g}^{0.370} = 0.51008 * 0.8764^{0.333} * 0.743^{0.370}$$

$$Nu_g = 0.437$$

$$As, Pr_g = \frac{\mu_g * c_{p,g}}{k_g} = \frac{287.95 * 10^{-3} * 1130}{0.0438} = 0.743$$

$$Nu_g = \frac{h_g * D_{h,g}}{k_g}$$

Where, $D_{h,g} = Hydraulic\ diameter\ in\ the\ gas\ side = 0.0068\ m$

$$h_g = \frac{Nu_g * k_g}{D_{h,g}} = \frac{0.437 * 0.0438}{0.0068} = 0.2815\ \text{W/m}^2\text{K}$$

Cold side calculation

$$\dot{M}_l = \frac{0.06765}{1} = 0.06765\ \text{kg/s per channel}$$

$$Re_l = \frac{C_{Re} * \dot{M}_l}{\mu_l} = \frac{3063.6 * 10^{-3} * 0.06765}{0.0027} = 76.76$$

$$Pr_l = \frac{\mu_l * c_{p,l}}{k_l} = \frac{0.0027 * 1925}{0.668} = 7.7807$$

So, the flow is in transient region.

$$Nu_l = 0.30541 Re_l^{0.580} Pr_l^{0.37} = 0.30541 * 76.76^{0.580} * 7.7807^{0.37}$$

$$Nu_l = 8.09$$

$$h_l = \frac{Nu_l * k_l}{D_h} = \frac{8.09 * 0.668}{0.0068} = 794.70\ \text{W/m}^2\text{K}$$

Wall resistance calculation

$$\frac{X_{wall}}{k_{wall}} = R_{wall} = \frac{0.6 * 10^{-3}}{16.85} = 35.6083 * 10^{-6}$$

$$\text{Plate thickness} = X_{wall} = 0.6 * 10^{-3} m$$

$$k_{wall} = 16.85\ W/mK$$

So,

$$\frac{1}{U_c} = \frac{1}{h_g} + \frac{1}{h_l} + \frac{X_{wall}}{k_{wall}} = \frac{1}{0.2815} + \frac{1}{794.70} + 35.6083 * 10^{-6}$$

$$\frac{1}{U_c} = 3.55$$

$$Or, U_c = 0.28\ \text{W/m}^2\text{K}$$

The heat transfer coefficient in the gas and liquid solution side has very large difference. As a result, the heat transfer resistances in the two sides of the heat exchanger have very high difference of magnitude. In this case, the heat exchange process will not be efficient. This is also evident from the low value of the overall heat transfer coefficient U_c.

From the above discussion it can be concluded that plate heat exchanger will not be suitable for this heat transfer application.

a = 0.96 b = 0.653 c = 1.471 d_H= 0.0068 C_{Re} = 3063.6

Heat Transfer	Pressure Drop
General	General
ıminar: Re < 8 $u = 0.51008\,Re^{0.333}\,Pr^{0.370}$	Laminar: Re < 28 $F_P = 5.2196\times10^{6}\,Re^{-1.00}$
ans I: 8 < Re < 115 $u = 0.30541\,Re^{0.580}\,Pr^{0.370}$	Trans I: 28 < Re < 185 $F_P = 1.3765\times10^{6}\,Re^{-0.60}$
ans II: 115 < Re < 160 $Nu = 0.68422\,Re^{0.410}\,Pr^{0.370}$	Trans II: 185 < Re < 430 $F_P = 0.2214\times10^{6}\,Re^{-0.25}$
Turbulent: Re > 160 $Nu = 0.14188\,Re^{0.720}\,Pr^{0.370}$	Turbulent: Re > 430 $F_P = 0.0892\times10^{6}\,Re^{-0.10}$
$\alpha_{is} = \frac{Nu.\lambda}{d_M}\,W/m^2.^oK$	$\Delta p_{is} = F_P \dot{M}^2 \rho^{-1} kPa$
Wall Viscosity Corrections $f_{is} = \left(\mu/\mu_w\right)^{\frac{0.3}{(Re+1)^{0.125}}}$	Wall Viscosity Corrections $\varphi_{is} = \left(\mu/\mu_w\right)^{\frac{-1}{(Re+1)^{0.5}}}$
	$\varphi_p = \frac{1.05}{0.95}$ from data sheet
Summary	Summary
$\alpha = \alpha_{is} f_{is}$ (General)	$\Delta p = \Delta p_{is} \varphi_s \varphi_p$ (General)
Plate Resistance $((m^2.^oK)/W)x10^4$	Subscript Notation;
AISI 316 0.6mm: 0.356 AISI 316 0.8mm: 0.475 Ti/TiPd 0.6mm: 0.259 Ti 0.8mm: 0.345 Inc 825 0.6mm: 0.442	***is*** = isothermal ***p*** = pressure

Table 1. Manufacturer's plate heat exchanger data sheet

1	Plate Area (A_{plate})	m^2	0.960		
2	Port Diameter or Equivalent	m	0.200		
3	Channel Width (b)	m	0.655		
4	Reynolds Number Coefficient (C_{Re})	-	3060		
5	Channel Type	-	L	M	H
6	Hydraulic Diameter (d_H)	m	0.0068	0.0068	0.0068
7	Velocity coefficient (C_U)	m^{-2}	450	450	450
8	Maximum number of channels when $n_s = 1$	-	230	300	470
9	Maximum number of channels when $n_s > 1$	-	130	175	270

	Channel Type		L		M		H	
10	Pressure Difference	bar	>1		>1		>1	
11	Correction Factor Over Pressure Side (ψ_p)	-	0.90		0.95		1.0	
12	Correction Factor Under Pressure Side (ψ_p)	-	1.10		1.05		1.0	

13	Inside Diameter	mm	0.200		
14	C_c – Values Straight Connection (In/Out)	-	0.0/0.0		
15	C_c – Values Elbow Connection (In/Out)	-			
16	C_c – Values Single Corner (In/Out)	-			
17	C_c – Values Double Corner (In/Out)	-			

18	Material	-	304/316		Ti/TiPd		Inc825
19	Plate Thickness (Xw)	mm	0.6	0.8	0.6	0.8	0.6
20	Wall Resistance	$10^4 m^2.{}^oK/W$	0.31	0.42	0.26	0.34	0.44

Table 2. Manufacture's mechanical data sheet

Conclusion

From the above analysis we can come to the conclusion that exhaust heat can be recovered effectively with help of a heat exchanger suitably designed for the purpose. It was also seen that a sufficiently high cooling load demand can be met with this recovered heat.

It was observed that a compact heat exchanger like plate fin heat exchanger would be best for this application.

The heat recovered in this heat exchanger is very less compared to the heat available. So there is sufficient scope of improvement over this design. However, improvement of heat transfer effectiveness will result in larger size of the heat exchanger. So a suitable tradeoff has to be done which will ensure proper running of the air conditioning system as well as be compact and lightweight.

The plate fin heat exchanger is susceptible to fouling. So, a filter has to be applied in the exhaust gas path upstream of the heat exchanger for reduction of soot and other particles. It will also help reduce the emission of air polluting particles. The filter will increase the flow resistance of the path and due to this the back-pressure in the engine will increase to certain extent. Because of this the power extracted from the engine per cycle would slightly decrease.

Novel refrigerants with improved characteristics can be used to further improve the performance and effectiveness of the heat recovery system.

The effect of installing a heat exchanger on the exhaust gas path would increase the flow resistance and back pressure to some extent. The change in combustion characteristics and efficiencies of the engine due to this change of pressure needs to be studied.

A part of the available cooling load can be used in pre-cooling of the incoming air fuel mixture. That will reduce the combustion temperature lowering the NO_X emission meet the latest EURO norms. For a supercharged engine, a part of the cooling load can be used to intercool the supercharged charge thus improving its performance.

References

1. Hatami, M., Ganji, D. D., & Gorji-Bandpy, M. (2014). A review of different heat exchangers designs for increasing the diesel exhaust waste heat recovery. *Renewable and Sustainable Energy Reviews*, *37*, 168-181.

2. Galindo J, Serrano JR, Climent H, Varnier O. Impact of two-stage turbocharging architectures on pumping losses of automotive engines based on an analytical model. Energy Conversion and Management 2010;51: 1958–1969.

3. Baines, N., Wygant, K. D., & Dris, A. (2010). The analysis of heat transfer in automotive turbochargers.*Journal of Engineering for Gas Turbines and Power*, *132*(4), 042301.

4. Dzida M, Mucharski J. On the possible increasing of efficiency of ship power plant with the system combined of marine diesel engine, gas turbine and steam turbine in case of main engine cooperation with the gas turbine fed in parallel and the steam turbine. Polish Maritime Research 2009;1(59)(vol. 16):47–52.

5. Wang SG, Wang RZ. Recent developments of refrigeration technology in fishing vessels. Renewable Energy 2005;30:589–600.

6. Shu, G., Liang, Y., Wei, H., Tian, H., Zhao, J., & Liu, L. (2013). A review of waste heat recovery on two-stroke IC engine aboard ships. Renewable and Sustainable Energy Reviews, 19, 385-401.

7. Maloney JD, Robertson RC. Thermodynamic study of ammonia-water power cycles. Oak Ridge (TN): Oak Ridge National Laboratory; 1953.

8. Kalinowski P, Hwang Y, Radermacher R. Waste heat powered absorption refrigeration system in the LNG recovery process. In: Proceedings of the 9th international sorption heat pump conference. Seoul, Korea; 2008.

9. Wang SG, Wang RZ. Recent developments of refrigeration technology in fishing vessels. Renewable Energy 2005;30:589–600.

10. Manzela, A. A., Hanriot, S. M., Cabezas-Gómez, L., & Sodre, J. R. (2010). Using engine exhaust gas as energy source for an absorption refrigeration system. *Applied energy*, *87*(4), 1141-1148.

11. Srikhirin, P., Aphornratana, S., & Chungpaibulpatana, S. (2001). A review of absorption refrigeration technologies. *Renewable and sustainable energy reviews*, *5*(4), 343-372.

12. Fernandez-Seara J, Vales A, Vazquez M. Heat recovery system to power an onboard NH_3–H_2O absorption refrigeration plant in trawler chiller fishing vessels. Applied Thermal Engineering1998;18:1189–205.

13. Kececiler A, Acar H, Dogan A. Thermodynamic analysis of the absorption refrigeration system with geothermal energy: an experimental study. Energy Conversion and Management 2000;41:37–48.

14. Hong, D., Chen, G., Tang, L., & He, Y. (2011). A novel ejector-absorption combined refrigeration cycle. *International Journal of Refrigeration*, *34*(7), 1596-1603.

15. Misra RD, Sahoo PK, Sahoo S, Gupta A. Thermoeconomic optimization of a single effect water/LiBr vapour absorption refrigeration system. International Journal of Refrigeration 2003;26:158–69.

16. Kizilkan O, Sencan A, Kalogirou A. Thermoeconomic optimization of a LiBr absorption refrigeration system. Chemical Engineering and Processing 2007;46:1376–84.

17. Talom, H. L., & Beyene, A. (2009). Heat recovery from automotive engine. Applied Thermal Engineering, 29(2), 439-444.

18. Garimella, S., Brown, A. M., & Nagavarapu, A. K. (2011). Waste heat driven absorption/vapor-compression cascade refrigeration system for megawatt scale, high-flux, low-temperature cooling. International Journal of Refrigeration, 34(8), 1776-1785.

19. Asdrubali, F., & Grignaffini, S. (2005). Experimental evaluation of the performances of a H_2O–LiBr absorption refrigerator under different service conditions. International journal of refrigeration, 28(4), 489-497.

20. Horuz, I. "Vapor absorption refrigeration in road transport vehicles." Journal of energy engineering 125.2 (1999): 48-58.

21. Peyghambarzadeh, S. M., Hashemabadi, S. H., Jamnani, M. S., & Hoseini, S. M. (2011). Improving the cooling performance of automobile radiator with Al_2O_3/water nanofluid. Applied thermal engineering, 31(10), 1833-1838.

22. Leong, K. Y., Saidur, R., Kazi, S. N., & Mamun, A. H. (2010). Performance investigation of an automotive car radiator operated with nanofluid-based coolants (nanofluid as a coolant in a radiator). Applied Thermal Engineering, 30(17), 2685-2692.

23. Pandiyarajan, V., Pandian, M. C., Malan, E., Velraj R., & Seeniraj, R. V. (2011). Experimental investigation on heat recovery from diesel engine exhaust using finned shell and tube heat exchanger and thermal storage system. *Applied Energy*, *88*(1), 77-87.

24. Zhang, H. G., Wang, E. H., & Fan, B. Y. (2013). Heat transfer analysis of a finned-tube evaporator for engine exhaust heat recovery. Energy Conversion and Management, 65, 438-447.

25. Ghazikhani M, Hatami M, Ganji DD, Gorji-Bandpy M, Behravan A, Shahi G. Exergy recovery from the exhaust cooling in a DI diesel engine for BSFC reduction purposes, Energy, Volume 65, 1 February 2014, Pages 44-51

26. Yang, F., Yuan, X., & Lin, G. (2003). Waste heat recovery using heat pipe heat exchanger for heating automobile using exhaust gas. Applied Thermal Engineering, 23(3), 367-372.

27. Mavridou, S., Mavropoulos, G. C., Bouris, D., Hountalas, D. T., & Bergeles, G. (2010). Comparative design study of a diesel exhaust gas heat exchanger for truck applications with conventional and state of the art heat transfer enhancements. Applied Thermal Engineering, 30(8), 935-947.

28.Zhang L.Z., Wang L.(1997). Performance estimation of an adsorption cooling system for automobile waste heat recovery.Applied Thermal Engineering Vol. 17, No. 12.pp. 1127-l 139.

29. Zhu R.Q., Han B. Q., Lin M. Z., and Yu Y. Z. Experimental investigation on an adsorption system for producing chilled water, Int. J. Refrigeration 15, 31-34 (1992).

30. Suzuki M. Application of adsorption cooling systems to automobiles. Heat Recovery Systems & CHP 13, 335-340 (1993).

31. Weng, C. C., & Huang, M. J. (2013). A simulation study of automotive waste heat recovery using a thermoelectric power generator. International Journal of Thermal Sciences, 71, 302-309.

32. Lu, H., Wu, T., Bai, S., Xu, K., Huang, Y., Gao, W. & Chen, L. (2013). Experiment on thermal uniformity and pressure drop of exhaust heat exchanger for automotive thermoelectric generator. Energy, 54, 372-377.

33. Love, N. D., Szybist, J. P., &Sluder, C. S. (2012). Effect of heat exchanger material and fouling on thermoelectric exhaust heat recovery. Applied Energy, 89(1), 322-328.

34. Duparchy A Leduc P, Bourhis G Ternel C. Heat recovery for next generation of hybrid vehicles: simulation and design of a Rankine cycle system. 3World Electric Vehicle 2009.

35. Sprouse, C., & Depcik, C. (2013). Review of organic Rankine cycles for internal combustion engine exhaust waste heat recovery. *Applied thermal engineering*, *51*(1), 711-722.

36. Chen H, Goswami DY, Stefanakos EK. A review of thermodynamic cycle and working fluids for the conversion of low-grade heat. Renew Sustain Energy Rev 2010;14:3059–67.

37. Wang Tianyou, Zhang Yajun, Peng Zhijun ,Shu Gequn.A review of researches on thermal exhaust heat recovery with Rankine cycle. Renew Sustain Energy Rev 2011;15:2862–71.

38. Saidur R. ,Rezaei M., Muzammil W.K., Hassan M.H., Paria S., Hasanuzzaman M. Technologies to recover exhaust heat from internal combustion engines. Renew Sustain Energy Rev2012;16:5649–59.

39. Conklin, J. C., & Szybist, J. P. (2010). A highly efficient six-stroke internal combustion engine cycle with water injection for in-cylinder exhaust heat recovery. Energy, 35(4), 1658-1664.

40. Wei H., Zhu T., Shu G., Tan L., Wang Y., Gasoline engine exhaust gas recirculation – A review, Applied Energy, Volume 99, November 2012, Pages 534-544

41. Zheng M ,Reader GT, Hawley JG. Diesel engine exhaust gas recirculation—a review on advanced and novel concepts. Energy Convers Manage 2004;45: 883–900.

42. Ghazikhani, M., Feyz, M. E., & Joharchi, A. (2010). Experimental investigation of the Exhaust Gas Recirculation effects on irreversibility and

brake Specific Fuel Consumption of indirect injection diesel engines. Applied Thermal Engineering, 30(13), 1711-1718.

43. C. P. Arora, Refrigeration and Air-conditioning (S. I. Units), Tata Mc Graw Hill Publishing Company Ltd

44. Edward F.Obert, Internal Combustion Engines and Air Pollution, Harper & Row Publishers

45. M.L.Mathur and R.P.Sharma, A course in Internal Combustion Engines; Dhanpat Rai & Sons, Delhi

46. V.Ganesan, Internal Combustion Engines; Tata MC Graw- Hill Publishing Company Ltd., Delhi

47. M. Necati Ozsik; Heat Transfer, A basic approach; Mc Graw Hill Book Company

48. ASHRAE Hand Book for fundamentals

49. Carrier System Design Hand Book

50. Sadik Kakac and Hongtan Liu; Heat Exchangers Selection, Rating and thermal Design.

51. N. Afgan and E.U. Schliinder ; Heat Exchangers: Design and Theory Sourcebook

52. Ramesh K. Shah, Dusan P. Sekulic; Fundamentals of Heat Exchanger Design

53. W. M. Kays, A. L. London; Compact heat exchangers; Mc Graw Hill Book Company

54.Y.A Cengel; Heat and mass transfer; Mc Graw Hill Book Company

55. ETSU; Compact heat exchangers, a training package for engineers
56. CARRIER SYSTEM DESIGN HANDBOOK